

**α/β -hydrolase domain containing 15 (*Abhd15*)-
A new Player in Adipogenesis**

Diploma Thesis

by

Evelyn Walenta



Graz University of Technology

Institute for Genomics and Bioinformatics

supervised by

Ass. Prof. Mag.rer.nat. Dr.rer.nat. Univ.-Doz. Juliane Bogner-Strauß

graded by

Dipl.-Ing. Dr.techn. Univ.-Doz. Karin Athenstaedt

STATUTORY DECLARATION

I declare that I have authored this thesis independently, that I have not used other than the declared sources / resources, and that I have explicitly marked all material which has been quoted either literally or by content from the used sources.

.....
date

.....
(signature)

Acknowledgement

At least since my attendance in Juliane's laboratory project it was clear for me: "This is the work I want to do for my diploma thesis!" and maybe even more important: "This is the PI and team I want to work with in the future!" As the institute for Genomics and Bioinformatics is not part of the faculty of Technical Chemistry, Chemical & Process Engineering and Biotechnology, Karin was so nice to take over the grading of my diploma thesis and therefore smoothed the way for me to write my diploma thesis on a faculty external institute. I can not say how thankful I am that both Karin and Juliane worked together so amicably and had the same expectations into the diploma thesis and myself. Lucky me, actually my expectations into my supervisor were even exceeded. There was no time when Juliane was not contactable, and sometimes I called her at very odd times, and there was no question she was not able to answer or to send me on the right way. Sometimes, when I was frustrated because of strange results, she taught me to see a positive side and built me up again, and sometimes, in the right moments, she pushed me to go on harder. Without this great support this work wouldn't have been able to be done like it lays here!

I'm also very thankful for the knowledge about fluorescence microscopy Dietmar Rieder taught me, and also for the great knowledge Andreas Prokesch shared with me. But I also have to mention the "leprechauns" of the laboratory, who were always there with a helping hand and saved me therefore to go crazy because of doing ten things at the same time. Thank you so much to Claudia Neuhold, Florian Stöger and Markus Wolf!

Furthermore I want to thank the Institute of Molecular Biosciences at the University of Graz, which opened their wide knowledge of protein assays to me. Here special thanks go to Susanne Grond. With her friendly help the lipase assays could be realized.

Not to forget, thanks to my friends, who understood that I tend to play "submarine" if I am stressed, but still always were available when needed and not angry if I was difficult to contact for some weeks.

Last but not least I also have to say thanks a million to David, who endured my mood swings, changing with the laboratory results, and also to my family, who carved my way of life. Without the inspiring example of my parents and my sister, but also because of my little brother, who always brought me back to the ground, it wouldn't have been possible for me to reach the mountain!

THANK YOU SO MUCH!!!

Abstract

Adipocyte differentiation is a highly regulated process which has been studied extensively during the last several years. Many regulatory factors have been characterized, but high-throughput technologies revealed that a lot of genes controlling adipogenesis remained unidentified. Transcriptome analysis of differentiating murine 3T3-L1 cells pinpointed one candidate gene annotated as *Abhd15* (α/β hydrolase domain containing 15). *Abhd15* is upregulated in various cell lines that undergo adipogenesis (murine, human and primary cells). Expression profiling of mice tissues showed that *Abhd15* is mainly expressed in brown adipose tissue (BAT), white adipose tissue (WAT), and liver. In both, BAT and WAT a decreased expression was detectable when fasted. However, the expression of *Abhd15* in WAT was neither significantly altered upon a chow diet or on a high fat diet in wild type mice nor in genetically obese mice.

Using fluorescence microscopy of Cos7 cells overexpressing *Abhd15* revealed that the protein is located in the endoplasmic reticulum. However, western blot analysis showed ABHD15 also to be secreted. The predicted hydrolase activity could be demonstrated, as ABHD15 shows phospholipase activity, enlightened by the release of free fatty acids from different phosphatidylcholins.

In addition, *Abhd15* was identified as a potential target gene of PPAR γ , the “master regulator of adipogenesis” because 1st: predicted PPAR γ binding sites were found on the *Abhd15* promoter, 2nd: the expression of *Abhd15* is significantly upregulated when treating differentiating 3T3-L1 cells with the PPAR γ agonist rosiglitazone and, 3rd: there is no expression of *Abhd15* in PPAR γ -ko mouse embryonic fibroblasts (MEFs).

These results argue that ABHD15 plays an important role in adipogenesis probably by providing a ligand for PPAR γ by its role as a phospholipase.

Contents

1	Abbreviations.....	3
2	Introduction.....	7
3	Materials & Methods.....	13
3.1	Materials.....	14
3.1.1	Cloning.....	14
3.1.2	Cell culture.....	14
3.1.3	RNA isolation.....	16
3.1.4	cDNA synthesis.....	16
3.1.5	qPCR.....	16
3.1.6	Oil red O staining.....	17
3.1.7	Protein quantification.....	17
3.1.8	Hydrolase/lipase assay.....	17
3.1.9	Western blot.....	18
3.1.10	Fluorescence microscopy.....	19
3.2	Methods.....	20
3.2.1	Cloning of <i>Abhd15</i> into the vectors pMSCVpuro and pHisMaxC.....	20
3.2.2	Cell culture.....	21
3.2.2.1	Handling.....	21
3.2.2.2	Differentiation.....	22
3.2.3	Transfection.....	22
3.2.4	Transduction.....	23
3.2.5	RNA isolation.....	23
3.2.6	cDNA synthesis.....	24
3.2.7	qPCR.....	24
3.2.8	Oil red O staining.....	25
3.2.9	Protein quantification.....	25
3.2.10	Hydrolase/lipase assay.....	25
3.2.11	Cell lysate, secreted protein and cell fractionation.....	26
3.2.12	Western blot.....	26
3.2.12.1	Gel electrophoresis.....	27
3.2.12.2	Transfer.....	27
3.2.12.3	Incubation.....	27
3.2.12.4	Exposure.....	28
3.2.13	Fluorescence microscopy.....	28

4	Results	29
4.1	Investigation of computationally gene predictions	30
4.2	Upregulation during murine and human adipogenesis.....	31
4.3	Expression in murine tissues.....	32
4.4	Influence of cell culture additives on <i>Abhd15</i> expression	34
4.5	<i>Abhd15</i> is a PPAR γ target.....	34
4.6	Silencing and overexpression of <i>Abhd15</i>	36
4.7	ABHD15 shows phospholipase activity	40
4.8	ABHD15 locates to the endoplasmatic reticulum and is secreted	42
5	Discussion	46
6	Figure Legends.....	51
7	References	54

1 Abbreviations

<i>Abhd15</i>	α/β -hydrolase domain containing 15 gene
ABHD15	α/β -hydrolase domain containing 15 protein
alpha	minimum essential medium alpha
aP2	adipocyte protein 2 (a carrier protein for fatty acids)
<i>Atgl</i>	adipose triglyceride lipase gene
BAT	brown adipose tissue
BMI	body-mass index
BSA	bovine serum albumine
cDNA	complementary DNA
C/EBP (α,β,γ)	CCAAT-enhancer-binding protein (α,β,γ)
CFP	cyan fluorescent protein
CHOP	transcript factor homologous to CCAAT-enhancer-binding proteins
CM	cardiac muscle
DAPI	4',6-Diamidino-2-phenylindol
DC	direct current
ddH ₂ O	double distilled H ₂ O
DEPC	diethylpyrocarbonate
Dex	dexamethasone
DM1	differentiation medium 1
DM2	differentiation medium 2
DMEM	Dulbecco's modified eagle medium
DMSO	dimethylsulfoxide
DNA	deoxyribonucleic acid
dNTP	deoxyribonucleotide triphosphate
dsDNA	double stranded DNA
DTE	dithioerythritol
DTT	dithiothreitol
EDTA	ethylenediaminetetraacetate
ER	endoplasmatic reticulum
FA	fatty acid
FBS	foetal bovine serum
FFA	free fatty acid
GATA 2/3	GATA-transcription factor 2/3
GFP	green fluorescent protein
HFD	high fat diet
His-Tag	codon for six histidines in a row
HSL	hormone-sensitive lipase

1 Abbreviations

IBMX	3-Isobutyl-1-methylxanthine
IGF1	insulin-like growth factor-1
Ind	induced
Ins	insulin
KLF	krüppel-like factor
ko	knock out
KROX20	early growth response protein-2
LCFA	long chain fatty acid
L-Glu	L-Glutamine
Liv	liver
LPA	lysophosphatidic acid
MCS	multiple cloning site
MEF	mouse embryonic fibroblast
MEM	minimum essential medium
mRNA	messenger RNA
ntc	non-targeting control
<i>ob</i>	obese gene
PBS	phosphate buffered saline
PBST	Tween including phosphate buffered saline
PC	phosphatidylcholine
PCR	polymerase chain reaction
PIC	protease inhibitor cocktail
PLA ₂	phospholipase A ₂ enzyme
pMSCV	plasmid murine stem cell virus
<i>Pparγ</i>	peroxisome proliferator-activated receptor γ gene
PPRE	peroxisome proliferator-activated receptor response elements
P/S	penicillin/streptomycin
qPCR	quantitative polymerase chain reaction
RAR	retinoic acid receptor
RNA	ribonucleic acid
Rosi	rosiglitazone maleate
RXR	retinoid X receptor
SGBS	Simpson-Golabi-Behmel syndrome
shRNA	short hairpin RNA
Sig	signal peptide
SM	skeletal muscle
<i>sn</i>	stereospecific numbering

1 Abbreviations

sPLA ₂	secreted phospholipase A ₂ enzyme
StdM	standard medium
SREBP1c	sterol regulatory element binding protein 1c
TF	transcription factor
TG	triglyceride
tRNA	transfer RNA
TZD	thiazolidinedione
WAT	white adipose tissue
wt	wild type
YFP	yellow fluorescent protein

2 Introduction

Obesity, medically described as a state of increased adipose tissue resulting in enhanced body fat and weight, rises to a worldwide health problem. For the last 20 years, the number of obese people, which means people of a Body-mass index (BMI = mass in kilogram divided by square of height in meters) of 30 or higher, has increased by 8 %, and the trend still goes on¹. Several studies showed that life expectancy is strongly reduced if the BMI lies significantly above the ideal level². The ideal BMI for women is 20-25 and 20-27 for men¹. Obesity promotes diseases like diabetes mellitus type II, hypertension, cardiovascular disease, and certain cancers. Hence, obesity leads to an increase of morbidity and mortality². Body weight and composition are determined by genetic, environmental and psychological factors. From the environmental point of view, we are living in a well-nourished society, combined with a reduced requirement for physical exertion. For sure, these are the ideal conditions for an over weight trend, but nevertheless most individuals are still lean and others obese. Obesity however, often is a result of genetic factors^{3,4}. Consequently, the complete understanding of adipogenesis, and therefore further identification and enlightenment of molecules and genes that influence adipogenesis, will lead to new options for the treatment of obesity.

What is known until now is that the growth of adipose tissue involves the increase in adipocytes size as well as the formation of new adipocytes from precursor cells⁵.

Among the mammalian species, two types of adipocytes are distinguishable, white and brown ones, which yield in white adipose tissue (WAT) and brown adipose tissue (BAT). In mice BAT differs from WAT in the location and the time of differentiation into mature adipocytes, as brown adipocytes differentiate before birth. In humans, BAT can be found in large depots in infancy, but only in small amounts and dispersed in the WAT of adults. Additionally, brown adipocytes store less lipid than white ones and hold more mitochondria (e.g. for heat production) and express almost all genes that are found in white adipocytes, and even some more⁶.

Adipocytes are specialized in synthesis and storage of big amounts of triglycerides (TGs). Therefore the function of adipocytes is thermal isolation⁷, but more to the point they are essential regulators of the whole-body energy homeostasis. Furthermore, fat cells secrete several proteins that regulate processes like adipogenesis and energy balance as well as haemostasis, blood pressure and immune function^{6,8}. One example, which shows how important these secreted factors are, is leptin, the obese gene (*ob*) product, which regulates the body fat mass by signalling satiety^{9,36}.

¹ http://apps.who.int/bmi/index.jsp?introPage=intro_3.html

2 Introduction

A scheme of the complete process of adipogenesis known from *in vitro* studies of fibroblasts and preadipocytes is shown in figure 1. It can be divided in two main phases, the determination and the terminal differentiation. In the phase of determination, pluripotent stem cells are converted into multipotent mesenchymal stem cells and subsequently into preadipocytes. These steps do not end up in any morphological changes, but afterwards the cells have lost their potential to differentiate into other cell types. During the terminal differentiation, the preadipocytes convert into mature adipocytes. This includes the appropriate characteristics like the machinery for lipid transport and synthesis, insulin sensitivity, and secretion of specific proteins⁶.

In the second phase of adipogenesis, the cells at least pass through growth arrest before the new phenotype comes up, characterized by chronological changes in gene expression. Interestingly cell confluence or cell-cell contact per se does not seem to be required for terminal differentiation but growth arrest. To acquire this status the transcription factor CCAAT-enhancer-binding protein (C/EBP) α and the peroxisome proliferator-activated receptor γ (PPAR γ) are cooperatively involved⁵. The expression of these two proteins plays a major role in regulation of adipogenesis and PPAR γ is also known as the “master regulator of adipogenesis”¹⁰. Subsequently to the growth arrest, a clonal expansion occurs to some preadipocyte models like 3T3-L1, but not to human cell lines. During this post-confluent mitosis, which conduces the examination of growth-related proteins and differs from pre-confluent cell growth, preadipocyte cell lines undergo at least one round of cell division^{5,6}.

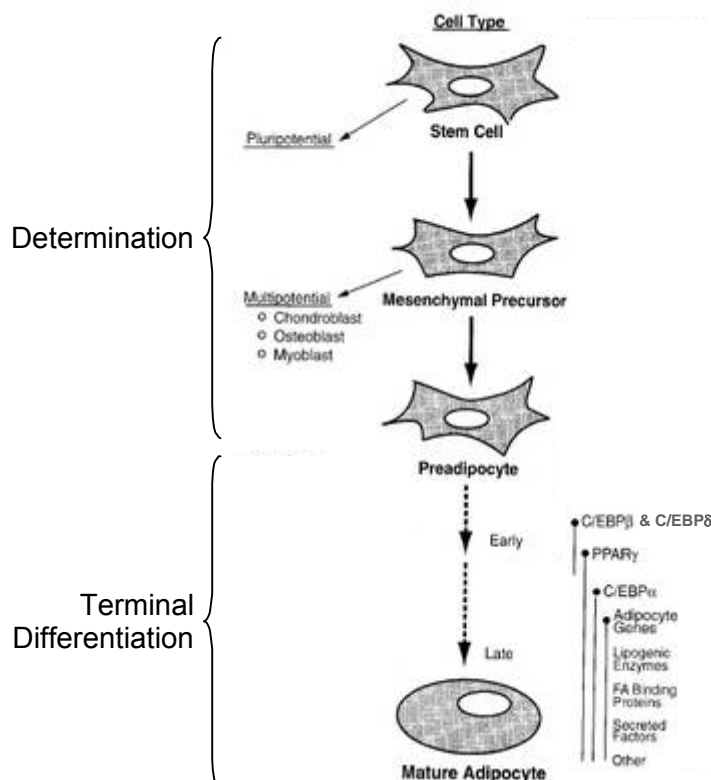


Figure 1: Adapted scheme of whole process of adipogenesis⁸

2 Introduction

Growth and differentiation of all animal cells are controlled by cell-cell and cell-extracellular environment communication. This communication operates with hormones and growth factors, acting via specific receptors to transduce external signals through a cascade of intracellular events. Hence, to induce terminal differentiation *in vitro* induction reagents are added. The agents which are commonly used for the 3T3-L1 cell line are insulin (Ins), which acts through the insulin-like growth factor-1 (IGF-1) and promotes lipogenesis and inhibits lipolysis, 3-isobutyl-1-methylxanthine (IBMX), a cyclic adenosine monophosphate (cAMP) inhibitor, and dexamethasone (Dex), a synthetic glucocorticoid agonist^{8,11}. Addition of these reagents evokes a lot of changes in gene expression. Most of the genes influenced during this process are transcription factors (TF) and although nowadays over 100 of TF are known to influence adipogenesis, the quest is still not at end (some of them are shown in figure 2).

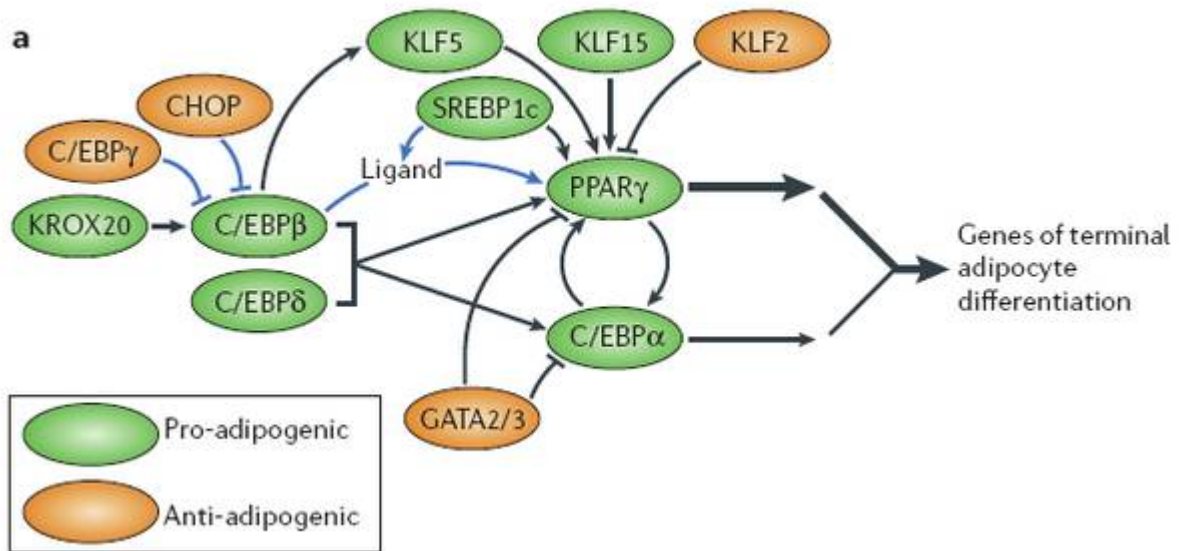


Figure 2: Draft of the transcriptional cascade in the terminal adipocyte differentiation⁶

The C/EBP family contains three of the most important adipogenic transcription factors, C/EBP α , C/EBP β , and C/EBP δ . The transiently increased expression of C/EBP β during the early terminal differentiation is induced by the early growth response protein-2 (KROX20)⁶, but somehow also by IBMX, whereas Dex induces the expression of C/EBP δ ⁸. It is known that C/EBP β homodimers induce the expression of PPAR γ , but apparently C/EBP β -C/EBP δ heterodimers are even more active¹². Furthermore, the early increased expression of C/EBP β -C/EBP δ leads to the induction of C/EBP α . All together, C/EBP β and C/EBP δ are identified as early TFs⁵. The level of C/EBP β decreases to 50% and C/EBP δ is nearly undetectable during the late differentiation, which highlights their enhancing function in the early terminal differentiation⁸. However, the expression of proteins, which are important for the maintenance of the fully differentiated adipocytes, remains on an increased level. Furthermore, C/EBP β and C/EBP δ are neither required nor sufficient for adipocyte

2 Introduction

differentiation, which is in contrast to PPAR γ and C/EBP α . However, the requirement of C/EBP α can be overcome by inducing agents^{5,6}. C/EBP α shows stimulation abilities for various adipocyte genes⁶, including for example two growth arrest-associated proteins GADD45 and p21^{13,14} and the adipocyte protein 2 (aP2), leptin, and insulin receptor proteins⁸.

Anyway, the member of the type II hormone receptor family PPAR γ is the major point of interest in adipogenesis⁶ since PPAR γ mainly regulates genes that control energy metabolism¹⁵. Many pro-adipocyte factors seem to function at least in part by activating the expression or activity of PPAR γ or by being activated by the latter⁶ (figure 2). For this reason, in search of novel adipogenic players the identification of PPAR γ targets is a good way to go¹⁶. PPAR γ occurs in a heterodimeric complex with a retinoid X receptor (RXR) and acts as a ligand activated transcription factor^{8,17,18,19}. Target genes of PPARs include a cognate DNA element called PPAR response element (PPRE), which is transcriptionally activated during adipocyte differentiation and has been identified in a number of adipocyte genes^{5,8,17}. On the other hand, the ligands of PPAR γ have a critical role in induction and maintenance of the adipogenic differentiation process. Although the major endogenous ligand is not known yet, synthetic and natural activators were identified, including some possibly indirect acting ones. Interestingly, all naturally occurring ligands are derived from arachidonic acid^{5,8,17}. Examples for synthetic activators are Thiazolidinediones (TZDs) which are used as drugs against type II diabetes²⁰. TZDs have proadipogenic properties on fibroblasts and myoblasts and the application increases insulin sensitivity⁸. The range of PPAR γ ligands is very broad. It stretches from some long chain fatty acids to fatty acid metabolites to eicosanoids^{5,17}. Some of these ligands like lysophosphatidic acid (LPA) have potent influences onto cell growth, mobility, differentiation, and adipogenesis^{21,37, 38}. Diverse as the ligands are the “producers” of these ligands. One out of them is the sterol regulatory element binding protein 1c (SREBP1c), a protein which increases fatty acid and fat synthesis. Hence, it is hypothesized to be involved in the generation of endogenous ligands of PPAR γ ²².

The overview of the different participants shows that adipogenesis is well explored, but the field of players is far from complete. High throughput techniques constantly bring up novel genes, whose expression is increased during adipocyte differentiation, indicating a role in adipogenesis²³. Transcriptome analyses of differentiating 3T3-L1 cells using microarrays²⁴ brought up the potential of the RIKEN clone 1300007F04²⁵ to be involved in adipogenesis. The final version of the murine mature RNA, translated into α/β -hydrolase domain containing 15 (ABHD15), was published in 2005²⁶. Enzymes with this typically secondary structure mostly show a central parallel or mixed β -sheet, surrounded by α -helices, which is called “canonical” α/β hydrolase fold (figure 3).

2 Introduction

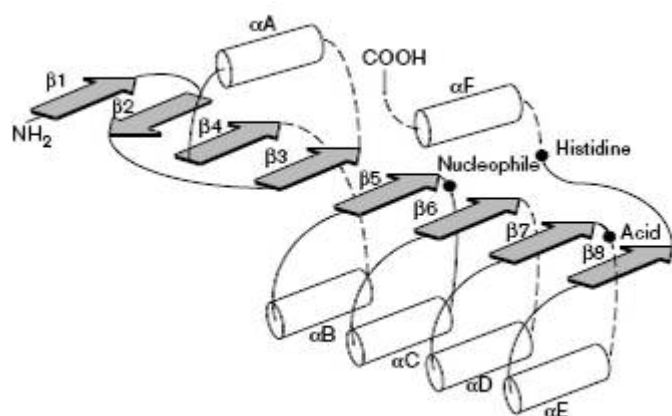


Figure 3: Diagram of the secondary structure of the "canonical α/β hydrolase" fold²⁷

Although the tertiary fold of the family members is the same, there are no obvious sequence similarities. Hence, this protein fold is one of the most versatile and widespread, reflected in the variety of enzyme classes, including lipases, esterases, dehydrogenases, dehalogenases, peroxidases, and epoxide hydrolases²⁸. To highlight how important some of these family members are, adipose triglyceride lipase (ATGL) should be mentioned, which plays a key role in TG breakdown in lipid droplet degradation²⁹. Knock down of *Atgl* leads to an increase of lipid droplet size³⁰ and further to concomitant excessive storage of TG to obesity³¹.

The knowledge of all the backgrounds noted above about ABHD15, its possible features and adipogenesis anyway, lead to the presumption of an important role of ABHD15 in cell development, adipogenesis. Maybe it could also be a weapon against obesity. Collectively, these data gave reason for investigating this gene in more detail.

3 Materials & Methods

3.1 Materials

3.1.1 Cloning

Aqua biodestillata sterile “Fresenius”, Fresenius

Diethylpyrocarbonate (DEPC) treated H₂O for molecular biology, Roth

DNA quantification Nano Drop ND – 1000 Spectrophotometer
Peqlab. Biotechnologie GmbH

linear DNA purification: “Pure Link^{TK} Quick Gel Extraction Kit”, Invitrogen corp.

One Shot® TOP10 chemically competent *E.coli*, Invitrogen corp.

Plasmid purification: “QIAprep Spin Miniprep Kit (250)”, Qiagen

PCR-primers: 5' + *Bgl*II restriction site ,Invitrogen corp.

CCG **AGA TCT** ATG CCT CCG TGG GCG GCC GCT

5' + *Bam*HI restriction site ,Invitrogen corp.

CGG **GAT CCC** CTC CGT GGG CGG CCG CTC TA

3' + *Xho*I restriction site ,Invitrogen corp.

CCG **CTC GAG** TCA CCG GGT GTA TGA ACG CTT CCA

3' + His-Tag + *Xho*I restriction site ,Invitrogen corp

CCG **CTC GAG** TTA ATG ATG ATG ATG ATG ATG -

CCG GGT GTA TGA ACG CTT CCA

Vectors: “pMSCVpuro”, Clontech Laboratories Inc.

“pHisMaxC”, Invitrogen

Restriction enzymes *Bam*HI, Fermentas

*Bgl*II, Fermentas

*Bsu*15I = *Cl*I, Fermentas

*Hind*III, Fermentas

*Xho*I, Fermentas

3.1.2 Cell culture

Cell lines: 3T3-L1 (mouse embryonic fibroblasts; adipose like)

OP9 (murine stromal cell line; able to differentiate into adipocytes)

Cos7 (fibroblasts, recovered from green vervet monkey)

SGBS (human Simpson-Golabi-Behmel Syndrome cells, adipose like)

Phoenix (human embryonic kidney cell line, retroviral expression system), gift of Gerald Höfler, Medical University of Graz

3 Materials & Methods

Chemicals: Dimethylsulfoxide (DMSO), Sigma-Aldrich Handels GmbH
KCl, Roth
KH₂PO₄, Roth
Na₂HPO₄*H₂O, Merck
NaCl, Roth
NaOH, Roth
Phosphate Buffered Saline (PBS 10x)
80 g NaCl, 2 g KCl, 11.5 g Na₂HPO₄*H₂O and
2 g KH₂PO₄ in 1 L ddH₂O; pH 7.4 with NaOH

Additives & Buffers: Dexamethasone (Dex), Sigma-Aldrich Handels GmbH
Foetal Bovine Serum (FBS), Invitrogen, Lot.Nr.:06G8151K
Hexadimethrine (Polybrene 8 mg/mL), Sigma-Aldrich Handels GmbH
3-isobutyl-1-methylxanthine (IBMX), VWR International
Insulin (Ins), Sigma-Aldrich Handels GmbH
Lentiviral particles ABHD15 "sc-108219-V", Santa Cruz
Lentiviral particles copGFP "sc-108080-Control", Santa Cruz
L-Glutamine (L-Glu) 200 mM, Invitrogen corp.
Metafectene, Biontex Laboratories GmbH
Normocin, Eubio
PBS pH 7.4, Invitrogen corp.
Penicillin/Streptomycin (P/S) Sol 10,000 U/mL / 10,000 µg/mL, Invitrogen corp.
Rosiglitazone Maleate (Rosi), Ebio
Trypsin/EDTA (10x) 0.5% Trypsin 5.4 mM EDTA*4NA, Invitrogen corp.
Puromycin dihydrochloride CELL CULTURE, Sigma-Aldrich H. GmbH

Culture media: standard medium (StdM): Dulbecco's Modified Eagle Medium
(DMEM) +4.5 g/L Glucose++, Invitrogen)
FBS 10%
Normocin 1:500
L-Glu 2 mM
P/S 100 U/mL / 100 µg/mL

MEMalpha (alpha): Minimum Essential Medium
(MEM) /alpha w/nucleosides, Invitrogen
FBS 20%
L-Glu 2 mM
P/S 100 U/mL / 100 µg/mL

3 Materials & Methods

Differentiation medium 1 (DM1): StdM

Dex 1 μ M

IBMX 0.5 mM

Ins 5 μ g/mL

Differentiation medium 2 (DM2): StdM

Ins 1 μ g/mL

3.1.3 RNA isolation

Cell culture cells: "Gen Elute™ Mammalian Total RNA Miniprep Kit", SIGMA
 β -Mercaptoethanol, Sigma Aldrich Handels GmbH

Mouse tissue: DEPC treated H₂O for molecular biology, Roth
Chloroform, Sigma-Aldrich Handels GmbH
TRIzol® reagent, Invitrogen corp.
Ethanol for molecular biology, GenXpress Service & Vertrieb GmbH
Isopropyl alcohol, VWR International (Merck, Margaritella)
Methanol, Sigma-Aldrich Handels GmbH

3.1.4 cDNA synthesis

Dithiothreitol (DTT) 0.1 M, Invitrogen corp.

5x First Strand Buffer, Invitrogen corp.

dNTP-Set 100 mM, PEQLAB Biotechnologie GmbH

Random Primer 3 μ g/ μ L, Invitrogen corp.

Super Script II Reverse Transcriptase 10,000 Units, Invitrogen corp.

3.1.5 qPCR

SYBR QPCR Supermix W/Rox, Invitrogen

qPCR-Primers: *Abhd15* murine, Invitrogen corp.

fw. TAT GAA CGT GGG TTC TTG CT

rev. TTG GTG TGA CAG AAC AGG GT

Abhd15 human, Invitrogen corp.

fw. CCG TGC TGC GCT GCC GAG AGT GG

rev. GGC TGT GGC ATA CCT GCT GAG GGC G

Atgl murine, MWG-biotech AG

fw. GTC CTT CAC CAT CCG CTT GTT

rev. CTC TTG GCC CTC ATC ACC AG

3 Materials & Methods

Tfll3 murine, Invitrogen corp.

fw. GTC ACA TGT CCG AAT CAT CCA

rev. TCA ATA ACT CGG TCC CCT ACA A

Ppar2 murine, Invitrogen corp.

fw. TGC CTA TGA GCA CTT CAC AAG AAA T

rev. CGA AGT TGG TGG GCC AGA A

ABI Prism 7000 Sequence Detection System

3.1.6 Oil red O staining

Formaldehyde, Sigma-Aldrich Handels GmbH

Isopropyl alcohol, VWR International (Merck, Margaritella)

Oil Red O, ICN

Oil red O stock: 0.25 g Oil Red O

50 mL Isopropyl alcohol

3.1.7 Protein quantification

“BCA Protein Assay Kit”, Pierce

3.1.8 Hydrolase/lipase assay

Bovine Serum Albumin (BSA), PAA Laboratories GmbH

CaCl₂, Sigma-Aldrich Handels GmbH

Diarachidinoyl-Phosphatidylcholine, Sigma-Aldrich Handels GmbH

Dipalmitoyl-Phosphatidylcholine, Sigma-Aldrich Handels GmbH

Dithioerythritol (DTE), VWR International (Merck, Margaritella)

Ethylenediaminetetraacetic acid (EDTA), Sigma-Aldrich Handels GmbH

Protease Inhibitor Cocktail Tablets (PIC), Roche Austria GmbH

NEFA-HR Test Reagent 1, Wako Chemicals GmbH

NEFA-HR Test Reagent 2, Wako Chemicals GmbH

Sucrose, Sigma-Aldrich Handels GmbH

Hormone-sensitive lipase (HSL)-assay buffer: 0.25 M Sucrose

1 mM EDTA pH 7.0

1 mM DTE

3 Materials & Methods

3.1.9 Western blot

Antibody 1: anti-His-Tag, Amersham Bioscience, Prod. Code: 27-4710-01

Antibody 2: Polyclonal Goat Anti-Mouse Immunoglobulins / HRP, DakoCytomation

Benzoase[®] Nuclease, Merck

Dithioerythritol (DTE), VWR International (Merck, Margaritella)

NuPAGE[®] 10% Bis-Tris Gel 1,0mmX 10 well, Invitrogen copr.

Glycerol 98%, Lactan

β-Glycerophosphate, Sigma-Aldrich Handels GmbH

LDS Sample Buffer 4x, Invitrogen corp.

Methanol, Sigma Aldrich Handels GmbH

NaF, International (Merck, Margaritella)

NuPAGE[®], MOPS SDS Running Buffer 20x, Invitrogen copr.

Orthovanadate, Sigma Aldrich Handels GmbH

Protease Inhibitor Cocktail Tablets (PIC), Roche Austria GmbH

Roentogen Liquid, Tetanal

Roentogen Superfix, Tetanal

Seebblue[®] Plus2 Prestained Standard, Invitrogen corp.

Sodium Dodecylsulfate (SDS), VWR International (Merck, Margaritella)

Super Signal West Pico, VWR International (Merck, Margaritella)

TGS-Buffer (10x), Bio-Rad Laboratories GmbH

Tris Ultra Quality, Lactan

Tween 20, VWR International (Merck, Margaritella)

PBST: Tween 20 0.05%

PBS

Blocking solution: BSA 5%

PBST

Lysis buffer: aqua biodesstillata ster. "Fresenius", Fresenius

glycerol 10% v/v

β-glycerophosphate 10 mM

NaF 10 mM

Na orthovanadate 100 μM

SDS 2.5% v/v

Tris-HCl 50 mM

Transfer buffer stock: Tris Ultra Quality 28 g

glycerol 143 g

distilled H₂O 1000 mL

3 Materials & Methods

Transfer buffer: Transfer buffer stock 10% v/v
 methanol 20% v/v
 distilled H₂O 1000 mL

3.1.10 Fluorescence microscopy

Antibody 1: anti-His-Tag, General Electric company
Antibody 2: donkey anti-mouse Alexa Fluor® 546, Invitrogen corp.
4',6-Diamidino-2-phenylindol (DAPI), Merck
Glutaraldehyde (GA), Sigma Aldrich Handels GmbH
Paraformaldehyde (PFA), Sigma Aldrich Handels GmbH
SlowFade Gold mounting medium, Invitrogen corp.
Triton X 100, Roth
Tween® 20, AppliChem GmbH

3 Materials & Methods

3.2 Methods

3.2.1 Cloning of *Abhd15* into the vectors pMSCVpuro and pHisMaxC

For these experiments the vectors pMSCVpuro and pHisMaxC were used. pMSCVpuro stands for “murine stem cell virus” and is a plasmid derived from the murine embryonic stem cell virus (MESC) and retroviral vectors. This vector can either be used for transient or stable transfection. The latter can be reached by transfecting Phoenix cells that are producing viral particles which can further be used for infection of various cell lines to generate cell lines stably expressing the gene of interest by Puromycin selection. pHisMaxC is a plasmid that was specially designed to enhance the protein expression in mammalian cells. Additionally, it offers the possibility of an N-terminal His-Tag, which means six histidine residues in a row, detectable by antibodies and chromatography columns.

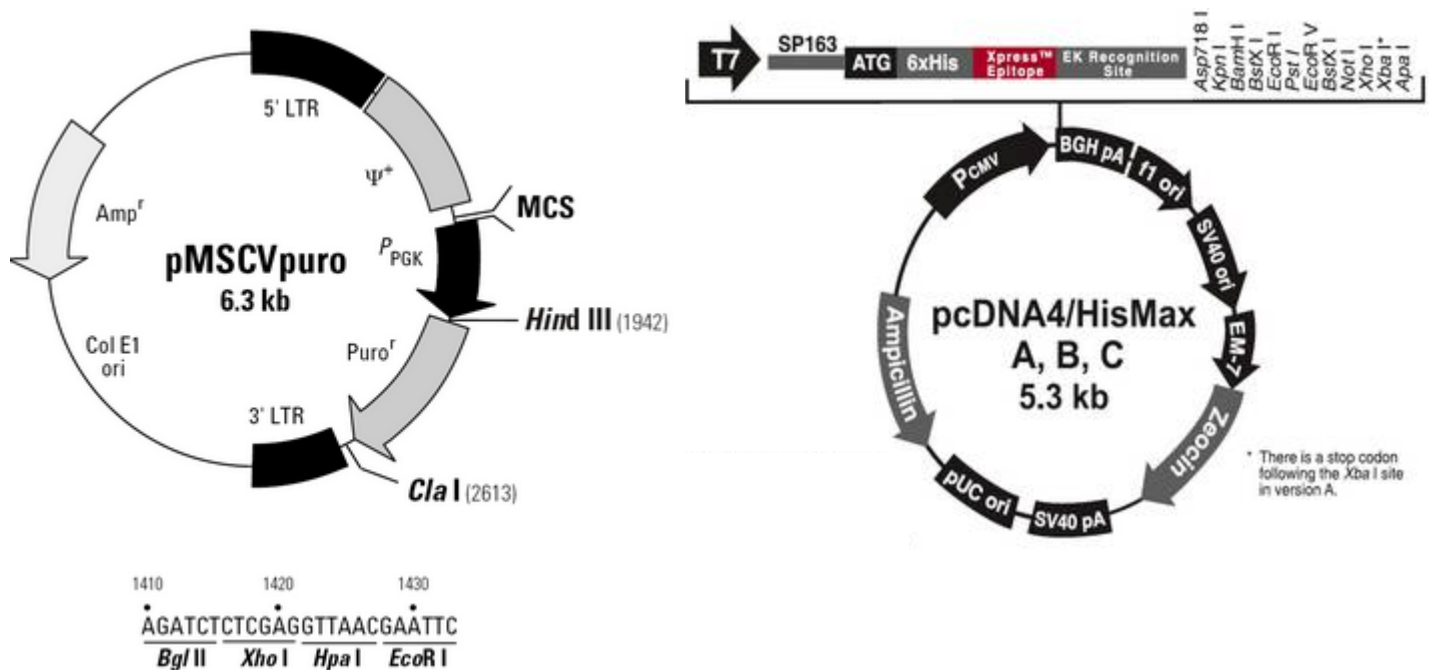


Figure 4: Vector maps of cloning plasmids pMSCVpuro and pHisMaxA,B,C

Both cloning vectors contain a multiple cloning site (MCS), restriction sites for various endonucleases, an origin of replication for bacterial growth and an ampicillin resistance for bacterial selection.

The coding sequence of murine *Abhd15* was amplified by PCR (polymerase chain reaction) using pfu polymerase (Fermentas). cDNA of differentiated 3T3-L1 cells (d4) served as template and primers including the restriction sites for *Bam*HI, *Bgl*II, *Xho*I and *Xho*I with His-Tag, were designed.

3 Materials & Methods

- 5'-CCG AGA TCT – *Abhd15* – CTC GAG CGG-3' for pMSCVpuro
5'- *Bgl*II – *Abhd15* – *Xho*I -3'
- 5'-CCG AGA TCT – *Abhd15* – 6x CAT – TAA CTC GAG CGG-3' for pMSCVpuro
5'- *Bgl*II – *Abhd15* ~~Stop~~ – His-Tag – Stop – *Xho*I -3'
- 5'-CGG GAT CC – *Abhd15* – CTC GAG CGG-3' for pHisMaxC
5'- *Bam*HI – ~~ATG~~ *Abhd15* – *Xho*I -3'

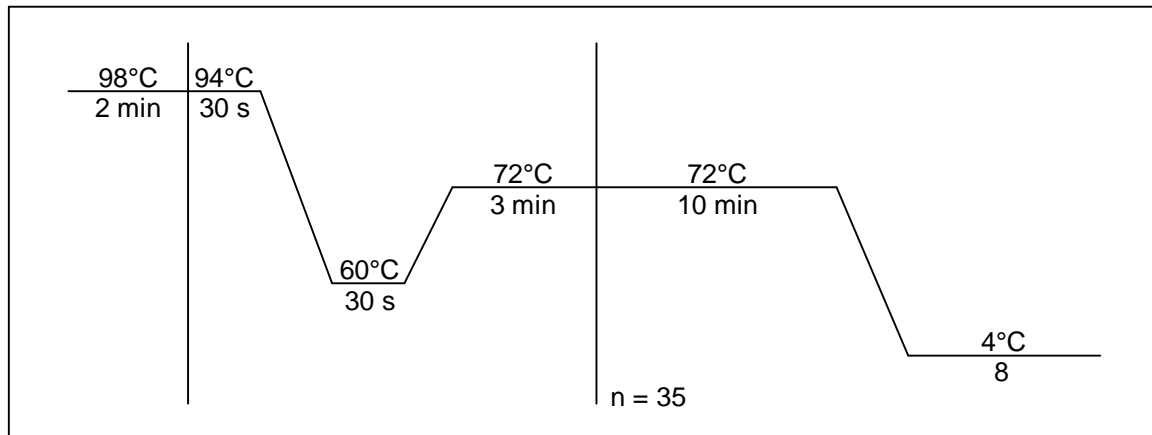


Figure 5: Temperature program for PCR

After the appropriate double digests, as recommended by fermentas^{II}, the products containing the whole reading frame were ligated into *Bgl*II-*Xho*I digested pMSCVpuro and *Bam*HI-*Xho*I digested pHisMaxC, using T4 ligase (New England Biolabs inc.). After transformation into *E. coli* Top10 cells for propagation and purification using a miniprep kit, control restriction digesting was done. Therefore the pMSCVpuro constructs were cut by *Cl*aI/*Xho*I and *Hind*III/*Bgl*II and the pHisMaxC construct by *Bgl*II/*Xho*I.

3.2.2 Cell culture

3.2.2.1 Handling

- Storage

To store cells for a longer period they were held deep frozen in liquid nitrogen tanks. To avoid cell death 10% of DMSO was added to the common media.

For defrosting the 1 mL cell amount had to be diluted very fast in a ratio of about 1:10 with fresh, prewarmed media. 24 h after the cell settlement the media was changed.

^{II} <http://www.fermentas.com/en/tools/doubledigest>

3 Materials & Methods

- Cultivation

3T3-L1 cells were cultivated in StdM (standard medium) and OP9 cells in alpha (MEMalpha). The change of media was done every 3 days.

- Splitting

To avoid total cell confluence, which is especially important for the 3T3-L1 cell line, they have to be split at 60-80% of confluence. Therefore the medium was sucked off, the cells were washed with PBS twice and trypsin solution was added (1 mL for a 75 mL growth plate) to disconnect the dish-cell interaction. Complete optimal medium was used to stop the reaction and to seed the cells into various dishes.

3.2.2.2 Differentiation

3T3-L1 cells were grown to confluence (day -2) and induced to differentiate using the standard hormonal cocktail (Differentiation Medium 1, DM1) on day 0. The media was changed to Differentiation Medium 2 (DM2) on day 3, to StdM on day 5 and from then on every 2 days.

The differentiation was also studied under different conditions of media. Therefore starting with day 0, Dex, IBMX and insulin (2 µg/mL) were added separately to the StdM. Furthermore the influences of 12 h and 24 h boosts of Rosiglitazone, Dex, IBMX and Insulin on *Abhd15* expression in fully differentiated cells were evaluated with qPCR.

3.2.3 Transfection

To transiently integrate foreign DNA into cos7 and Phoenix cells, the plasmids were transfected using metafectene. This transfection reagent changes the DNAs to compact structures to ensure the easy entry into the cell, and in addition, it destabilises the lipid membrane coating the DNA/RNA by repulsive electrostatic forces to provide it in better accessible conditions.

One hour before transfection, the StdM had to be changed to StdM without FBS. For each 6-well 1 µg DNA and 4.5 µL metafectene per 1 µL DNA were added to 50 µL SM without FBS each and were mixed together gently. For negative controls an empty vector was transfected. After 20 min of rest the metafectene-DNA cocktails were pipetted dropwise into the growth media over the cells (not directly on the cells!). The StdM without FBS was changed to StdM after 4 h and the maximum expression was reached after 48-72 h.

The expression products were used for further experiments. The transfection of cos7 with the pHisMaxC-*Abhd15* and pMSCVpuro-*Abhd15*-HisTag constructs lead to increased protein expressions and therefore they were used for Protein-Assays, cell fractionation and western

3 Materials & Methods

blots. The transfection of Phoenix cells with pMSCV-*Abhd15* lead to amphotropic lentiviral particles in the supernatant, which were collected and used further on for transduction.

3.2.4 Transduction

The common procedure to stably integrate foreign DNA into the genomic DNA of 3T3-L1 cells is transduction using lentiviral particles as carriers.

3T3-L1 cells were seeded into 6 well plates and transduction was started at about 40% confluence. To increase the effectivity of retroviral infection, polybrene (6 µg/mL at the final concentration) was added to the StdM. Polybrene is a polycation that neutralizes the charge interactions between the pseudoviral capsid and the sialic acid of the cellular membrane.

To achieve stable overexpression of *Abhd15* in these cells, 1 mL of the lentiviral particles containing supernatant from transfected phoenix cells mixed with 1 mL of StdM was used for transduction. For stable silencing of *Abhd15*, 3T3-L1 cells were infected with either 10 or 20 µL of *Abhd15* shRNA lentiviral particles and copGFP-control. As excessive exposure of polybrene can be toxic to cells the media had to be changed after an overnight incubation. For stable selection, puromycin was added to the StdM in a final concentration of 3 µg/mL for at least 5 days. After the death of non-transduced cells, the remaining 3T3-L1 cells were transferred to a 75 mL-flask with fresh StdM.

3.2.5 RNA isolation

Cell culture cells: After washing the cells with PBS twice the “Gen Elute™ Mammalian Total RNA Miniprep Kit” was used for RNA isolation. In contrary to the kit-directions the column bound RNA was resuspended in 30 µL DEPC treated H₂O for 1 min, centrifuged for 1 min at 15,700 g and eluted again with the same solution by centrifugation.

Mouse tissue: For homogenization, 1 mL TRIzol® reagent was added to the sample for each 100 g of mouse tissue. To avoid overheating, the tubes were kept on ice. The homogenized samples were incubated at room temperature for 5 min and afterwards chloroformed with 0.2 mL per each mL TRIzol® reagent to separate RNA, DNA and protein phases. After well-mixing for 15-20 s and calm down for 3 min at room temperature, the samples were centrifuged at 4°C and 12,000 g for 10 min. After centrifugation 3 phases were discernable. The colourless phase on the top contains RNA and has to be pipetted off very cautiously. The red coloured phase indicates DNA and the white one

3 Materials & Methods

contains proteins. After adding 0.5 mL isopropyl alcohol per each mL TRIzol® reagent, the samples were vortexed, incubated at room temperature for 10 min and centrifuged at 4°C and 12,000 g for 10 min. The supernatant was discarded and 1 mL ethanol was added per each mL TRIzol® reagent. Subsequently the samples were vortexed and centrifuged at 4°C and 7,500 g for 5 min. The supernatant was discarded and the residual pellets were dried depending on the size (5-30 min). The RNA was suspended by 25 µL DEPC treated H₂O per each mL TRIzol® reagent.

The RNA concentration was measured by a Nano Drop Spectrophotometer and stored at -80°C. For using the obtained RNA for qPCR it was reverse transcribed to cDNA.

3.2.6 cDNA synthesis

1 µg of tRNA, 1 µL dNTP mix and 300 ng Random Primers were filled up to 12 µL with DEPC treated H₂O, heated to 65°C for 5 min to destroy the secondary structure and subsequently chilled on ice. After addition of 4 µL 5x First Strand buffer and 2 µL 0.1 M DTT, the samples were gently mixed and incubated at 37°C for 2 min. 1 µL of the reverse transcriptase “SuperSript II” was added and the samples were incubated at 25°C for 10 min and subsequently at 37°C for 50 min. The reactions were inactivated at 70°C for 15 min and afterwards stored at -80°C.

3.2.7 qPCR

The polymerase chain reaction (PCR) allows to manifold exactly defined DNA sequences up to 3 kbp, with special polymerases even up to 40 kbp. Quantification of these sequences (qPCR) requires a fluorescent, in this case SYBR-green. SYBR-green absorbs blue light at a maximum wavelength of 498 nm and emits green light at a maximum wavelength of 522 nm when bound to double stranded DNA (dsDNA). Fluorescence increases proportionally to the formatted dsDNA amount. It has to be said that the DNA quantification works correctly only during the exponential production.

For each qPCR run there were used 4.5 ng cDNA solved in 4.5 µL H₂O sterile, 4.5 µL of 800 nM Primers and 9 µL SYBR green.

3 Materials & Methods

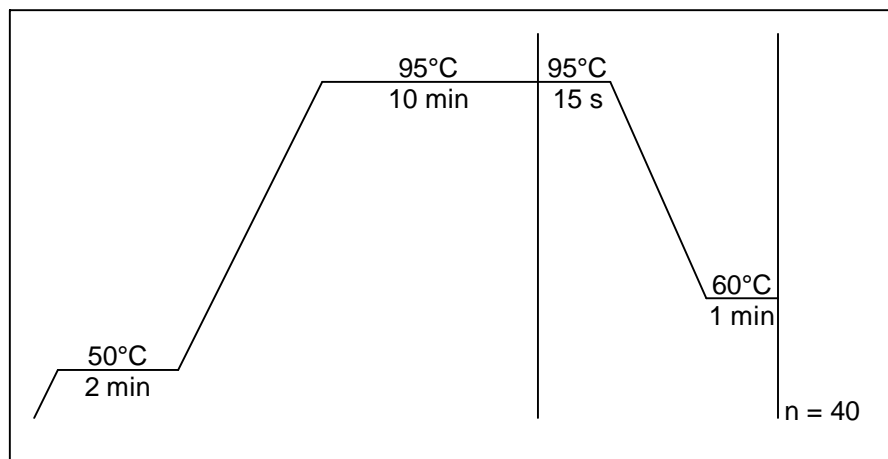


Figure 6: Temperature program for qPCR

3.2.8 Oil red O staining

The cells were washed with PBS twice and subsequently fixed with formaldehyde (10%) for 30 min. The Oil Red O stock is ready for use when diluted with ddH₂O (6:4) and filtrated through filter paper (1, Ø 110 mm). After sucking off the formaldehyde, the Oil Red O dye was pipetted onto the cells and incubated for 1 h. The fixed and dyed cells were stored covered with ddH₂O.

3.2.9 Protein quantification

For the quantification of proteins “BCA Protein Assay Kit”, produced by Pierce, was used.

3.2.10 Hydrolase/lipase assay

For the prove of phospholipase activity of ABHD15 the degradation of Dipalmitoyl- and Diarachidinoyl-Phosphatidylcholine (PC) into free fatty acids was observed. This was done by NEFA-HR (2) test by Wako Chemicals GmbH, which determines the quantity of released free fatty acids.

For obtaining the proteins in solution the cultured cells were washed with PBS twice, scrubbed off the plate with HSL-assay buffer and denaturated with ultrasound (2x 5 s; 44 J; amplitude 19) on ice. Afterwards the solution was centrifuged at 4°C for 5 min and 1,000 g to separate the membrane fragments and the DNA (pellet). The protein amount in the supernatant was detected by using “BCA Protein Assay Kit” and subsequently the solution was used for the hydrolase/lipase assays. 100 µg of protein were diluted to 50 µL with HSL-assay buffer and pipetted into a microtitre plate. After the addition of 100 µL of phospholipid substrate solution, which contained 0.3 mM phospholipid (PC), 3 mM CaCl₂, 2 % BSA and Tris-HCl-Buffer (50 mM; pH 7.0), the samples were incubated for 1 h at 37°C. Two 50 µL

3 Materials & Methods

units of each sample were transferred to fresh microtitre plates as technical replicates. After adding 75 μ L of NEFA-HR Reagent 1 the samples were incubated for 10 min at 37°C, followed by the addition of 150 μ L NEFA-HR Reagent 2 and an incubation of 10 min and 37°C. Finally the absorption was measured at a wavelength of 562 nm.

3.2.11 Cell lysate, secreted protein and cell fractionation

For obtaining the cell proteins in solution, the cultured cells were washed with PBS twice, scrubbed off the plate with 50 μ L Lysis Buffer for each 6-well and quantified using the “BCA Protein Assay Kit”. In addition, the supernatant of cos7 cells, transiently expressing His-tagged ABHD15, was collected by incubating the cells with serum-free medium for 6 h (48 h after transfection). To concentrate the extracellular proteins, the supernatant of the cells were nearly dried completely by a speed vac and resuspended in 30 μ L Lysis Buffer.

To enlighten the localization of ABHD15 in the cell, a cell fractionation was done. For this purpose cos7 cells, transiently expressing the His-tagged ABHD15 (72 h after transfection), were washed twice and scratched off the plate in PBS. After a centrifugation at 1000 g and 4°C for 10 min the cells were denaturated with ultrasound (3x 20 s) on ice. To obtain the nucleus the solution was centrifuged at 1,000 g and 4°C for 15 min. The nucleus was resuspended in 50-100 μ L Western blot Lysis Buffer. The supernatant was centrifuged at 100,000 g and 4°C for 60 min to separate cytoplasm and membrane fraction. The membrane pellet was solved in 80 μ L Western blot Lysis Buffer with PIC and 200 μ L of the cytoplasm fraction was concentrated by evaporation and dissolved with 25 μ L Western blot Lysis Buffer with PIC.

During the working process the protein solutions were kept on ice and stored at -20°C for longer periods. Cell lysate, supernatant and all three fractions of the cell fractionation were investigated for ABHD15 expression by western blotting.

3.2.12 Western blot

A benzoase digest was done to achieve an easier handling of the samples. For this purpose the protein solutions were inactivated at 94°C for 4 min and subsequently chilled back to room temperature. After the addition of 1 μ L benzoase, the samples were incubated at room temperature for 1 h and centrifuged for 2 min at 13.000 g. If there had been a visible pellet after centrifugation a separation of the supernatant would have been necessary. In these cases the samples contained just small quantities of DNA, though enough to make the protein solutions chewy without the benzoase digest.

3 Materials & Methods

3.2.12.1 Gel electrophoresis

To separate proteins because of their different charge and size a gel electrophoresis was done. For this purpose 5-10 μg intracellular proteins, 1-2 μg extracellular proteins, collected as mentioned before, and 25 μL of the cell fractions (nuclei, membranes and cytoplasm) were used. The Biorad western blot chamber was filled with the gels and 700 mL of the diluted NuPAGE[®] buffer. Before loading, the samples, 10 μL 4x LDS and 1 μL DTE were filled up to 40 μL with H_2O sterile, mixed, incubated for 10 min at 70°C to denaturize the proteins and transferred into the gel slots. As a standard 10 μL of Seebblue[®] Plus2 mixed with 20 μL sterile H_2O and 5 μL 4x LDS was used.

The gel was run for about 1 h at 175 V constant DC.

3.2.12.2 Transfer

To run immuno-assays the proteins have to be transferred to a membrane. This can be done by charge, because in an electric field proteins move to the negative pole.

The membrane was activated in dd H_2O for 30 s. Afterwards filter papers, membrane, gel and felt were sucked with transfer buffer, laid on top of each other and fixed with a transfer plate (figure 7). The construct/pile was transferred into the transfer chamber, which was filled up with transfer buffer and an ice block. The transfer was done for 1.5 h at 120 V.

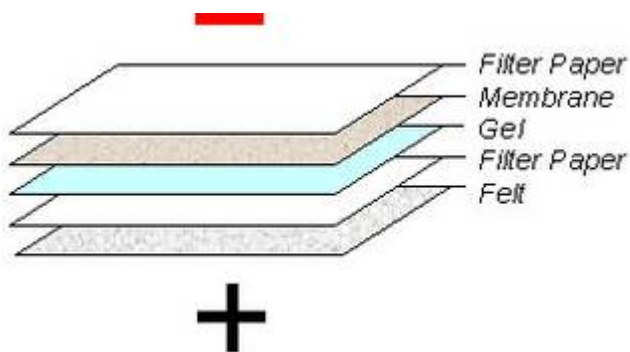


Figure 7: Construction for wet western blot transfer

To prevent the antibodies from binding to the membrane instead of the antigen, the membrane was blocked for 1 h in the blocking solution, followed by a triple wash in PBST.

3.2.12.3 Incubation

The membrane was incubated with two antibodies. The first one, the anti His-Tag (1:6000 in PBST), which binds selectively to the His-Tag, was used at 4°C over night on the 360° slide. After a triple wash with PBST the second antibody, anti mouse (1:3000 in PBST), was added at room temperature for 2 h on the 360° slide to bind to the anti His-Tag antibody. Finally, the membrane was washed three times in PBST.

3 Materials & Methods

3.2.12.4 Exposure

1.5 mL of each of the “Super Signal West Pico” solutions were mixed, pipetted onto the membrane and incubated for 5 min. To avoid the drying of the membrane, it was kept in a cling film for the rest of the handling. The fluorescing of the antibodies hit the photo paper (exposure time depending on fluorescing intensity), which was developed with Roentogen Liquid and Roentogen Superfix and finally washed with ddH₂O.

3.2.13 Fluorescence microscopy

The cos7 cells were seeded and grown on cover slips (corning #1.5) in 6 well plates. At 80 % confluence, they were transfected with 1 µg of the pHisMaxC-*Abhd15* construct and 0.5 µg of *D1er*. *D1er* is an ER FRET (fluorescence resonance energy transfer) sensor which consists of CFP (cyan fluorescent protein) and YFP (yellow fluorescent protein) versions which are linked by a mutated Calmodlin Ca²⁺ binding domain. The ER targeting is achieved by a 5' calreticulin signal sequence and a 3' KDEL (Lys-Asp-Glu-Leu) sequence.

An empty pHisMaxC vector was transfected for negative control. 48 h after transfection the cover slips were removed from the medium and prepared for imaging.

For high resolution 3D imaging the cells were fixed with freshly prepared 2% paraformaldehyde and 0.2% glutaraldehyde in PBS for 15 min, then washed three times with PBS, permeabilized for 5 min with 0.2% Triton-X 100 in PBS and finally washed again three times in PBS. An antibody was used for immuno detection of the His-Tag. The antibody was diluted 1:200 in 4% BSA / 0.1% Tween20 / PBS, applied to the cells and incubated over night at 4°C. As an additional control, the cells were incubated without the addition of antibody one. Subsequently the cells were washed three times with PBS and incubated for 1 h at room temperature with an anti-mouse antibody, including a fluorophor, which was diluted like antibody 1. The nuclei were counterstained for 5 min with 0.05 µg/mL DAPI in PBS. Finally the cover slips were mounted on microscopy slides with approximately 5 µL mounting medium.

All images were collected on a Zeiss AxioImager Z1 epifluorescence microscope equipped with a Zeiss AxioCam MRm CCD camera using a 63x 1.4 NA objective lens.

4 Results

4.1 Investigation of computationally gene predictions

Abhd15 is conserved in the genome of mice, humans, chimpanzee, dogs, rats and zebrafish^{III}. The phylogenetic tree of the nucleotide sequences of humans, chimpanzee, mice, rats, and dogs (figure 8), created with the European Bioinformatics Institute tool ClustalW2^{IV}, shows the high homology of the *Abhd15* cDNA in different mammals.



Figure 8: Phylogenetic tree of *Abhd15* cDNA of different mammals

Mice and rats are in common use as experimental models. Figure 9 shows that the murine model is a better analogon to the human being than the rat model.

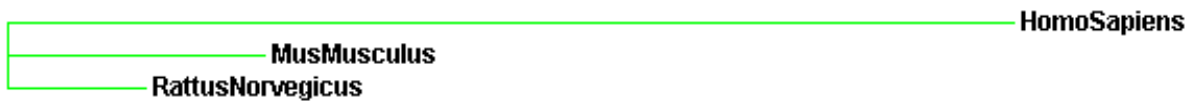


Figure 9: Phylogenetic tree of *Abhd15* cDNA of humans, mice, and rats

The UniProtKB/Swiss-Prot database^V rendered that the ABHD15 murine protein (459 amino acids) belongs to the α/β hydrolase and esterase-lipase superfamilies. Hence to these structure similarities a carboxylesterase activity is very likely. As a charge relay system the amino acids 351 and 382, which are aspartic acid and histidine, are presumed to be active sites.

In addition, comparisons of ABHD15 with amino acid sequences out of UniProtKB/Swiss-Prot database showed that ABHD15 has potential to be secreted as there is a predicted extracellular signal peptide region.



Figure 10: Predicted superfamily and signal peptide (Sig) domains of ABHD15

^{III} [http://www.ncbi.nlm.nih.gov/sites/entrez?Db=homologene&Cmd=Retrieve&list_uids=12142&log\\$=seqview_homolog](http://www.ncbi.nlm.nih.gov/sites/entrez?Db=homologene&Cmd=Retrieve&list_uids=12142&log$=seqview_homolog)

^{IV} <http://www.ebi.ac.uk/Tools/clustalw2/index.html>

^V <http://www.uniprot.org/>

4 Results

4.2 Upregulation during murine and human adipogenesis

Gene expression of *Abhd15* was assessed in various murine cell lines. *Abhd15* was strongly upregulated during adipogenic differentiation in both, murine cell lines and primary cells, namely 3T3-L1 and OP9 cells as well as mouse embryonic fibroblasts (MEFs) (figure 11). The results are mean values (\pm standard deviation) of three independent experiments except the MEFs, which show one representative experiment.

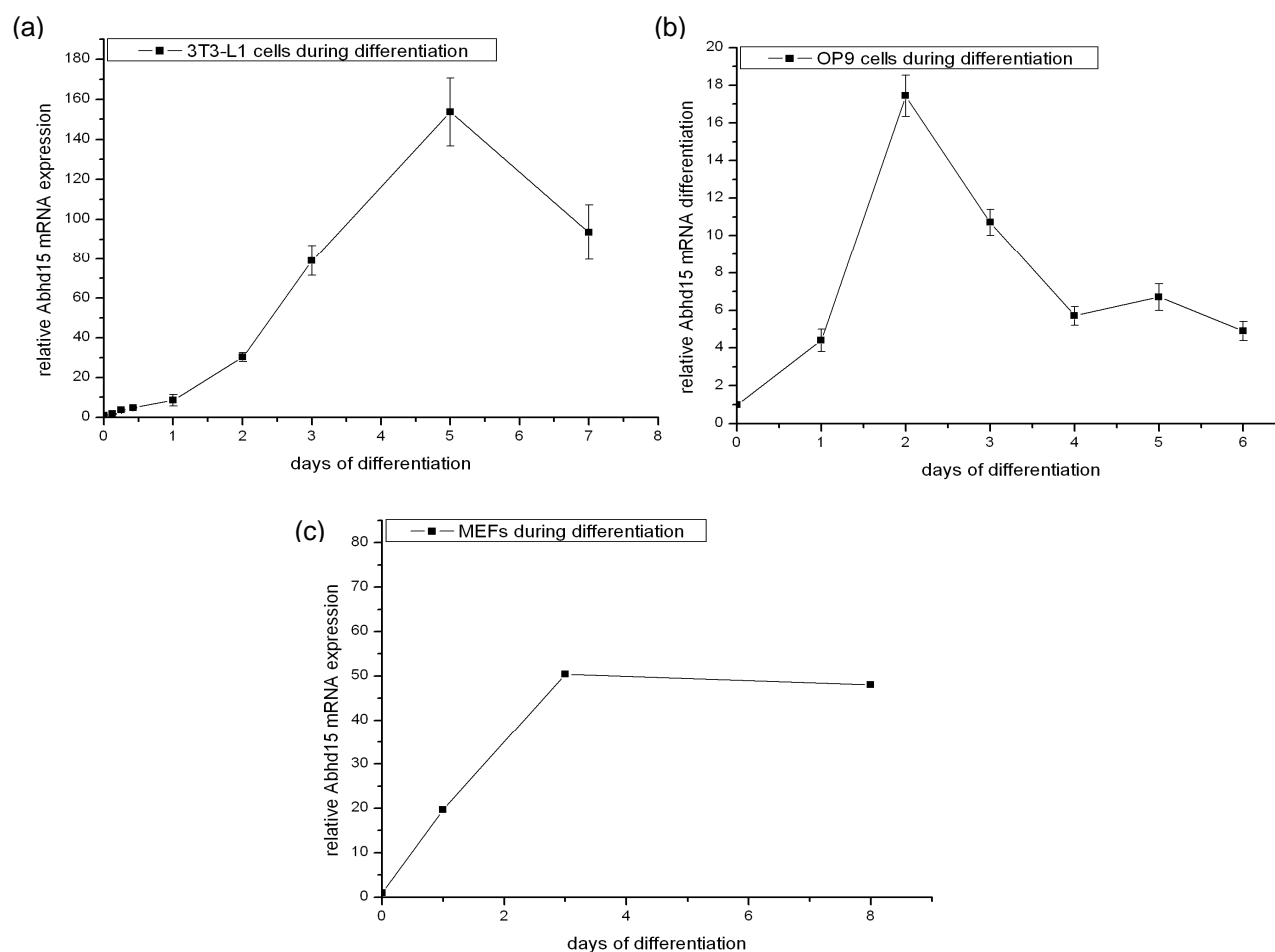


Figure 11: *Abhd15* expression during differentiation of (a) 3T3-L1 fibroblasts, (b) OP9 cells and (c) MEFs

A similar expression profile of the human orthologous gene of *Abhd15* (NM_198147) could be shown in the human Simpson-Golabi-Behmel syndrome (SBGS) cells (figure 12), which are preadipocytes isolated from the adipose tissue of patients with SBGS and a very useful and common tool in adipogenic studies³².

4 Results

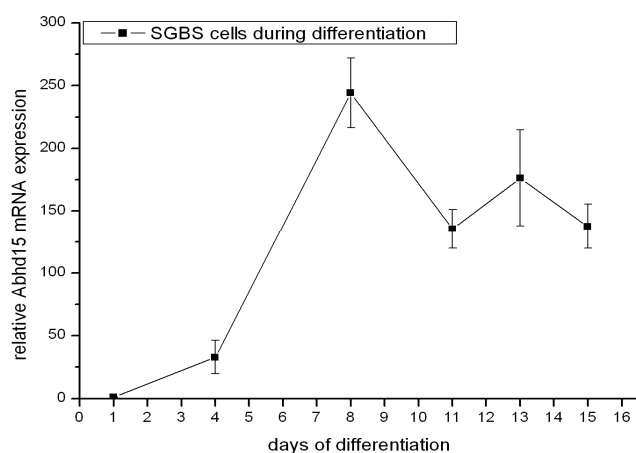


Figure 12: *Abhd15* expression during differentiation of SGBS cells

The expression profiles of *Abhd15* received from murine and human cell lines and primary cells that undergo adipogenesis are comparable as shown in figures 11 and 12. During the first days of differentiation the expression of *Abhd15* is strongly increased followed by a light decrease and subsequently stays at a constant level.

Overall, these data indicate that the level of *Abhd15* expression is upregulated during adipogenesis in mice and men suggesting a potential role in the fat cell development process.

4.3 Expression in murine tissues

qPCR experiments showed that the highest expression of *Abhd15* can be found in the brown adipose tissue (BAT), followed by the white adipose tissue (WAT), and the liver (Liv). There is hardly any expression detectable in the skeletal muscle (SM) and cardiac muscle (CM) (figure 13).

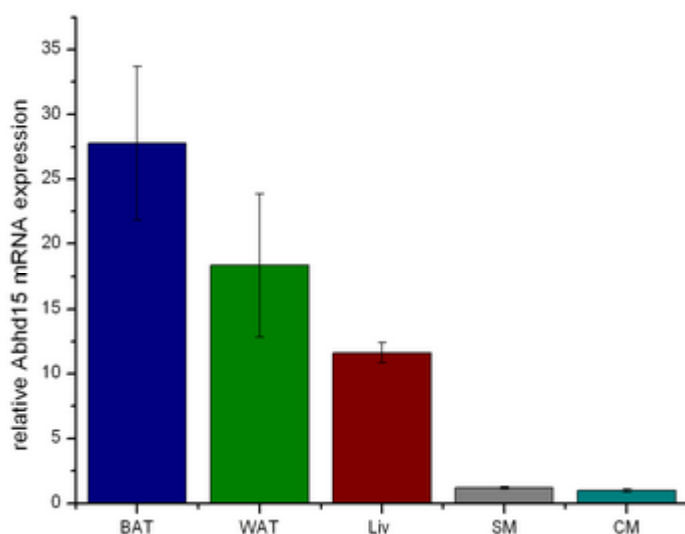


Figure 13: Expression of *Abhd15* in murine tissues

4 Results

To evaluate whether *Abhd15* is upregulated in genetically obese mice (*ob/ob*) at the age of 3-4 months compared to their wild type littermates, qPCRs of WAT and Liv were carried out. Unexpectedly, there was no increase of *Abhd15* expression in the WAT of obese mice, whereas the expression of *Abhd15* in the Liv of *ob/ob* mice was about doubled (figure 14).

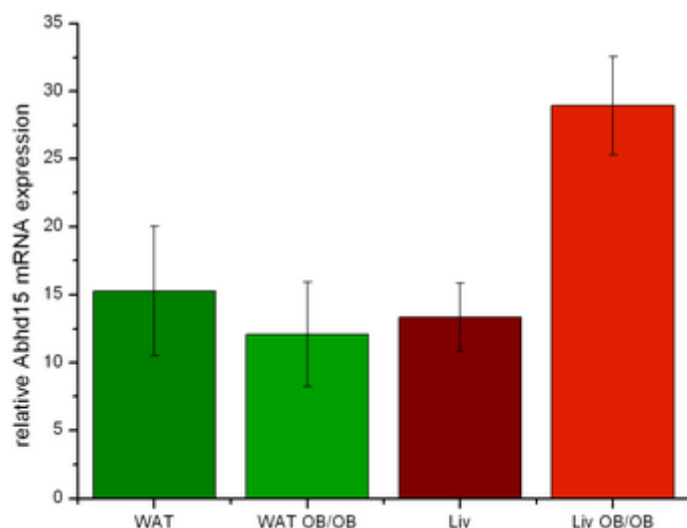


Figure 14: Expression of *Abhd15* in WAT and Liv of wild type and genetically obese (*ob/ob*) mice

Furthermore, we wanted to investigate whether food access or a special diet influence the expression pattern of *Abhd15*. In contrast to mice fed ad libitum, overnight fasted mice showed a slight decrease of *Abhd15* expression in BAT and WAT (figure 15a). However, mice on a high fat diet (HFD: 40% calories in fat) showed only a small reduction of *Abhd15* expression in the WAT on the short-term (7 weeks) and on the long-term (14 weeks) challenge on this diet. Compared to overnight fasted mice, which were refed 1 h before death, the mice which were fasted for 24 h showed a slightly lower expression of *Abhd15* (figure 15b).

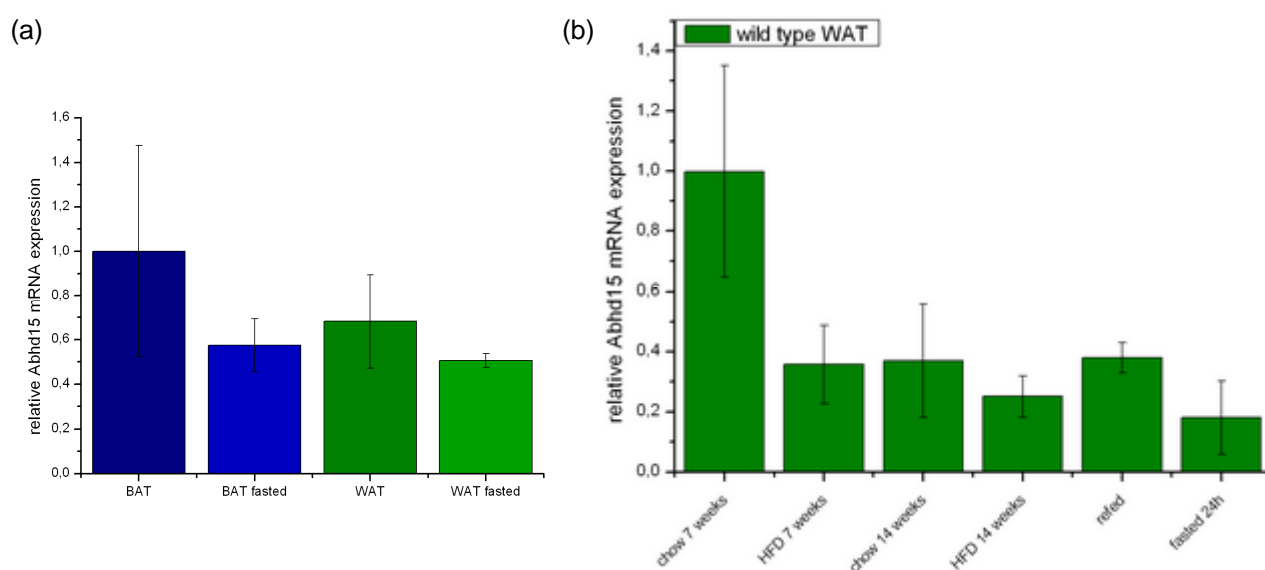


Figure 15: Comparison of *Abhd15* expression in mice on various diets

4 Results

4.4 Influence of cell culture additives on *Abhd15* expression

As shown before differentiation of 3T3-L1 cells lead to a strong induction of *Abhd15* expression. To evaluate whether the addition of Dexamethasone (Dex), 3-Isobutyl-1-methylxanthine (IBMX) or insulin (Ins) alone has an influence on *Abhd15* expression, cells were grown to confluence and 2 days later the various reagents were added for seven days. The treated cells were reaped seven days after starting the individual treatments. Whereas the expression of *Abhd15* was 2.5-fold higher in 3T3-L1 adipocytes treated with the standard differentiation cocktail, IBMX alone could not evoke a significant increase of *Abhd15* expression compared to non induced cells. Addition of Dex or Ins led to a small increase of *Abhd15* expression in comparison to control cells. (* $p \leq 0.05$, ** $p \leq 0.001$)

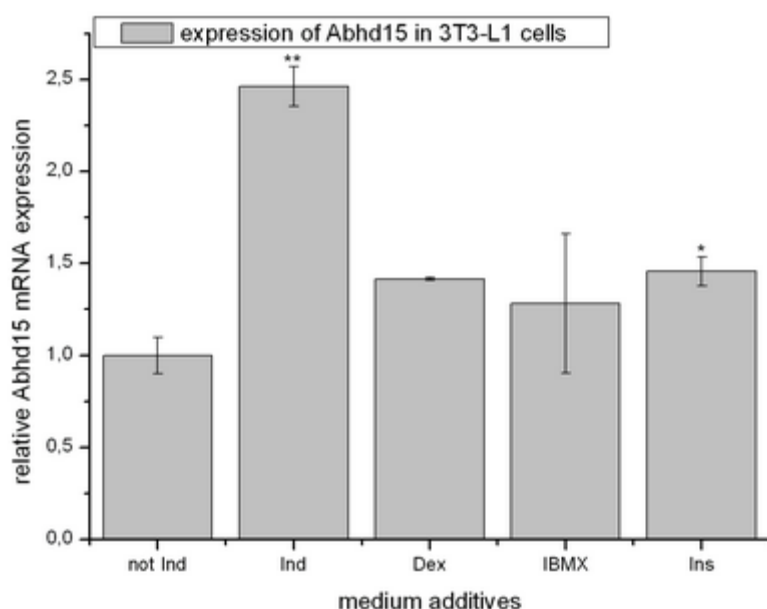


Figure 16: *Abhd15* expression after 7 days of treatment of 3T3-L1 cells with various additives

4.5 *Abhd15* is a PPAR γ target

Since we and others³³ found predicted PPAR γ binding sites on the *Abhd15* promoter, we wanted to evaluate whether a PPAR γ agonist can influence *Abhd15* expression. For this purpose, the differentiation of 3T3-L1 cells was persecuted with and without the addition of the Thiazolidinedione (TZD) PPAR γ agonist Rosiglitazone (Rosi) to the standard differentiation cocktail. As shown in figure 17 *Abhd15* expression was at least increased 4.5-fold from day 3 on when Rosi was added during the differentiation process. Thus it can be concluded that *Abhd15* expression is induced by PPAR γ activation.

4 Results

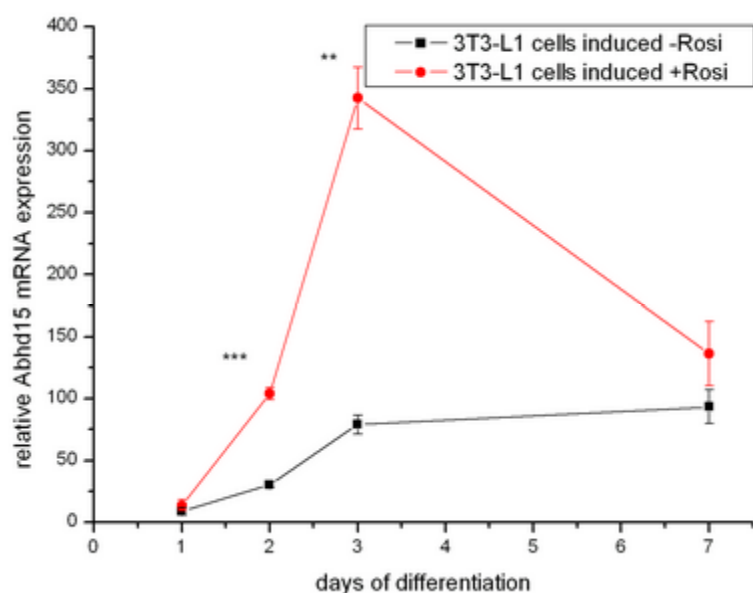


Figure 17: *Abhd15* expression during differentiation with and without addition of Rosi (1 μ M)

To evaluate whether short term treatment with the PPAR γ agonist also has an influence on the expression of *Abhd15*, fully differentiated 3T3-L1 adipocytes were treated with two concentrations (1 μ M and 5 μ M) of Rosi for 12 and 24 hours. mRNA levels of *Abhd15* were increased significantly upon treatment with 1 μ M Rosi after 12 hours (1.8-fold) and 24 hours (2.3-fold) compared to normally differentiated 3T3-L1 cells. However, the treatment with 5 μ M Rosi did not show a higher effect than with 1 μ M (figure 18). Thus in fully differentiated cells the Rosi dependent increase of *Abhd15* expression is time but not dose dependent.

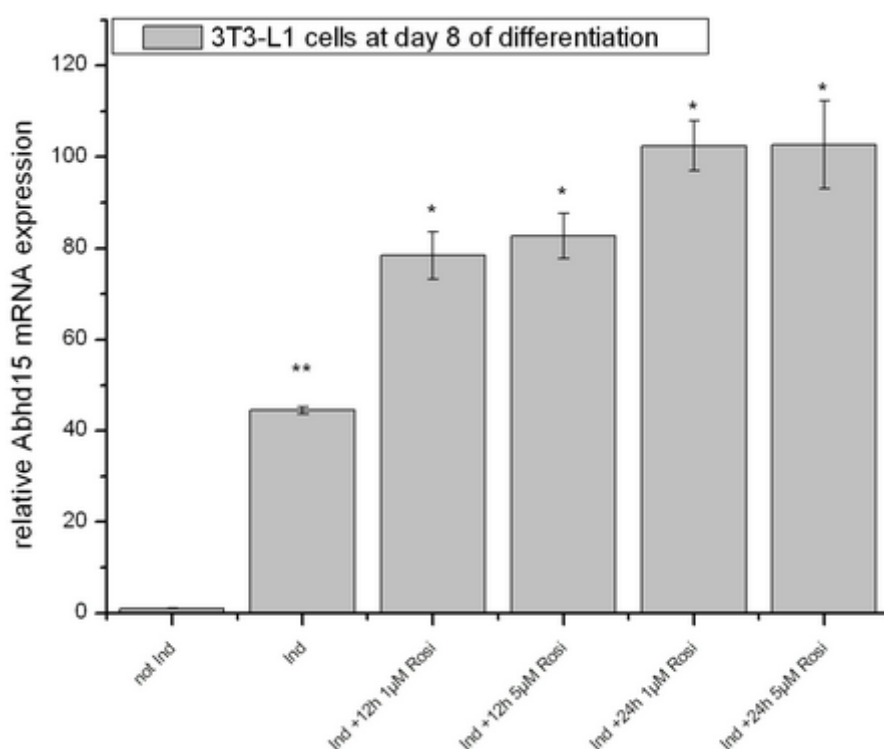


Figure 18: *Abhd15* expression during short term treatment of fully differentiated 3T3-L1 cells with Rosi

4 Results

These results provide strong evidence that *Abhd15* expression is subject to PPAR γ -dependent regulation, thus confirming the interaction between PPAR γ and *Abhd15* suggested by promotor studies.

To investigate further whether *Ppar γ* is required for the expression of *Abhd15*, MEFs from *Ppar γ ^{-/-}* and *Ppar γ ^{+/-}* mice were used and subjected to hormone-induced adipocyte differentiation. While *Ppar γ ^{+/-}* showed a significant increase of *Abhd15* mRNA expression during differentiation, *Ppar γ -knockout (ko)* MEFs did not. Furthermore, the addition of Rosi to *Ppar γ ^{+/-}* MEFs at day 4 of differentiation increased *Abhd15* expression 6-fold, whereas in *Ppar γ ^{-/-}* MEFs even upon addition of Rosi no expression of *Abhd15* could be observed (figure 19). These results show that *Ppar γ* is a prerequisite for *Abhd15* expression and that, as expected, Rosi can only increase *Abhd15* expression combined with the presence of *Ppar γ* .

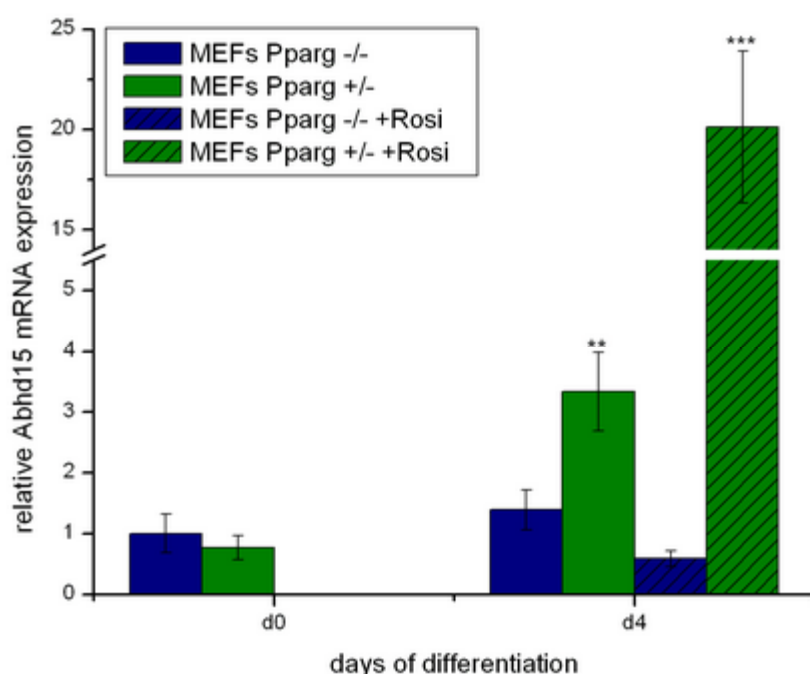


Figure 19: *Abhd15* expression in *Ppar γ ^{-/-}* and +/- MEFs

4.6 Silencing and overexpression of *Abhd15*

To gain more insight into the function of ABHD15 in adipocytes, silencing of *Abhd15* in 3T3-L1 cells was evaluated. For that purpose, *Abhd15* targeted shRNA (Santa Cruz), encoded by lentiviral vectors, was used to generate stably transduced cell lines with constitutive silencing of *Abhd15* expression. After transduction the cells were grown to confluence and induced to differentiate using the standard hormonal cocktail (Dex/IBMX/Ins). Unfortunately the shRNA lentiviral constructs only showed about 20% of *Abhd15* silencing capacity during differentiation in comparison to a non-targeting control (ntc) (figure 20). Hence, further

4 Results

experiments did not seem to be useful and the silencing has to be repeated in the near future.

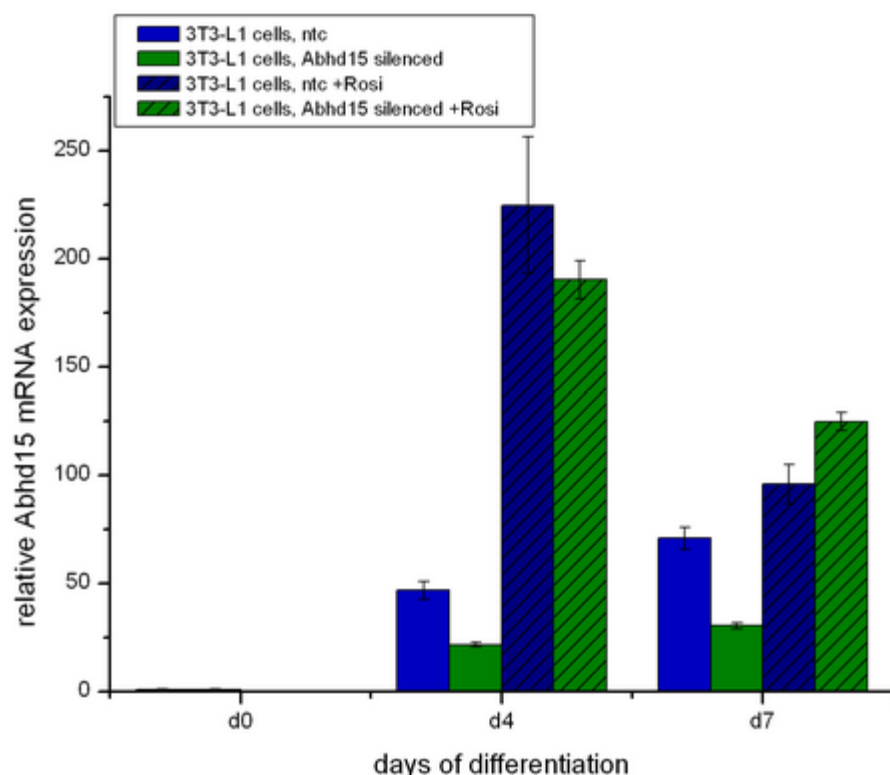


Figure 20: *Abhd15* expression of *Abhd15* silenced cells during differentiation

For overexpression of *Abhd15* in 3T3-L1 cells the pMSCVpuro-*Abhd15* construct was prepared as mentioned above. After ligation of the *Abhd15* gene, equipped with a forward *Bgl*II and a reverse *Xho*I restriction site by PCR (electrophoresis gel of double digested insert and vector see figure 21a) into the pMSCVpuro vector, a transformation of *E. coli* Top10 cells was done, providing twelve ampicillin resistant colonies. The following control restrictions identified five colonies as pMSCVpuro-*Abhd15*. Digesting the miniprep DNAs with *Bgl*II and *Xho*I showed that the *Abhd15* gene (1.4 kbp) was inserted into the five MSCV plasmids (6.3 kbp) (figure 21b). Furthermore the restriction of the five positive miniprep DNAs with *Hind*III and *Bgl*II provided one fragment of 5.5 kbp and one fragment of 1.9 kbp, which proved the results of the first control restriction digest (figure 21c). Control digest number three, done by *Cl*I and *Xho*I, manifested the other two, as there was one fragment of 1.2 kbp and another one of 6.5 kbp. None of the five constructs showed a fragment of 5.1 kbp which would represent the empty vector (figure 21d). For better understanding of the exonuclease digests the vector map of the plasmid including the *Abhd15* insert is shown in figure 22.

4 Results

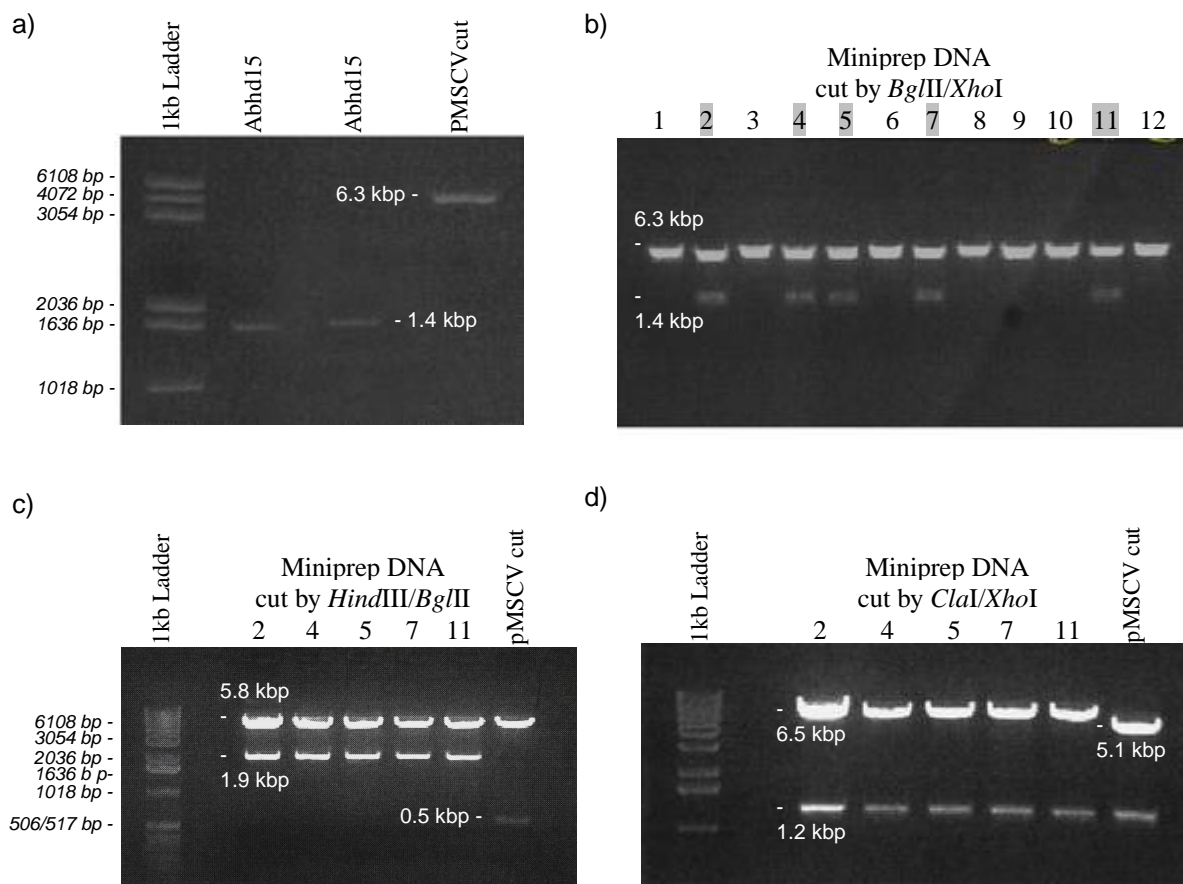


Figure 21: Electrophoresis gels of pMSCVpuro-*Abhd15* preparation

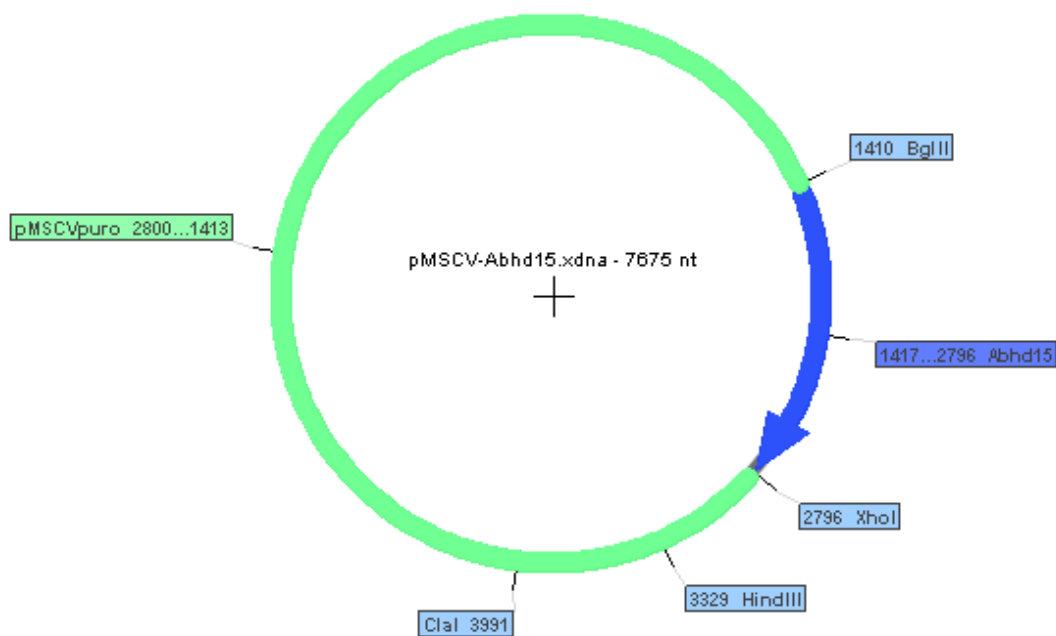


Figure 22: Vector map of the pMSCVpuro-*Abhd15* construct, including the restriction sites for control cuts

4 Results

After transfection of Phoenix cells with the obtained pMSCVpuro-*Abhd15* constructs, 3T3-L1 cells were stably transduced with the received amphotropic lentiviral particles as described above.

Next in line, we examined whether stable expression of *Abhd15* promotes adipogenesis in 3T3-L1 cells by stimulating them with different induction cocktails and measuring lipid accumulation by oil red O staining at day 7 of differentiation.

3T3-L1 cells overexpressing *Abhd15* showed a 200-fold increase of *Abhd15* mRNA expression, in comparison to cells expressing the pMSCVpuro control vector, which encouraged to use these cells for further experiments. Addition of Rosi to the standard hormonal cocktail (Dex/IBMX/Ins) showed a further increase of *Abhd15* expression. This matched to cells induced without Rosi as expected. But apparently, only a small further increase was possible. Anyway, no significant difference in lipid droplet content using Oil red O stainings could be recognized. Surprisingly the induction with Dex (1 μ M) evoked a fast and large lipid droplet formation, followed by the nearly all-embracing death of the cells within four days. The mRNA expression of *Abhd15* on Dex treated cells was also impressive. Interestingly the abounding Dex influence could not be recognized on standard induced *Abhd15* overexpressing 3T3-L1 cells, which were treated with the same Dex concentration, but additionally with IBMX and Ins. In contrast, *Abhd15* stably expressing cells induced with Ins (2 μ g/mL) and IBMX (0.5 mM) alone did not show any significant differences to the undifferentiated cells, with regard to oil red O stainings and relative mRNA expressions (figure 23).

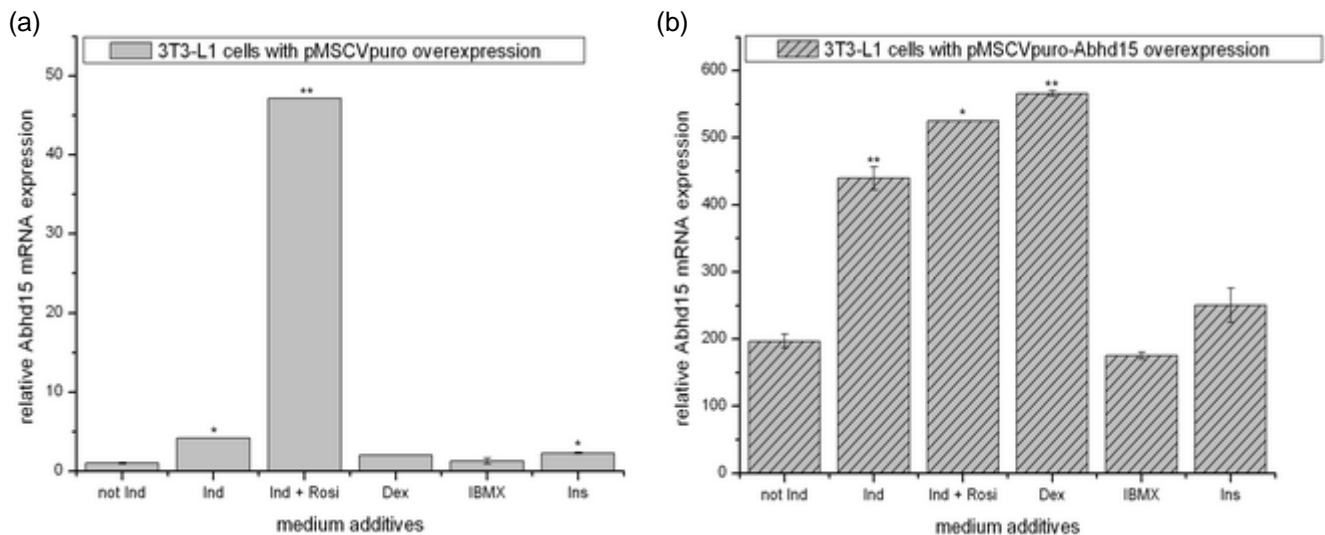


Figure 23: Stable overexpression of (a) pMSCVpuro and (b) pMSCVpuro-*Abhd15* in 3T3-L1 cells treated with different media for 8 days

On the whole it can be said that *Abhd15* overexpressing cells show a completely different reaction at treatment with Dex, which has to be investigated in further experiments in the near future.

4 Results

4.7 ABHD15 shows phospholipase activity

As there is a lipase activity of *Abhd15* predicted, it was tested if the mRNA expression of *Abhd15* increases, when an important triglyceride lipase gene like the adipose triglyceride lipase (*Atgl*) is knocked out, to take over part of triglyceride (TG) activity. Therefore tissues of *Atgl*-knockout mice were examined.

The investigation of *Atgl* knockout mice compared to wild type mice showed about 50% less expression of *Abhd15* in BAT and WAT in different diet stadia and nearly no difference in the liver (figure 24).

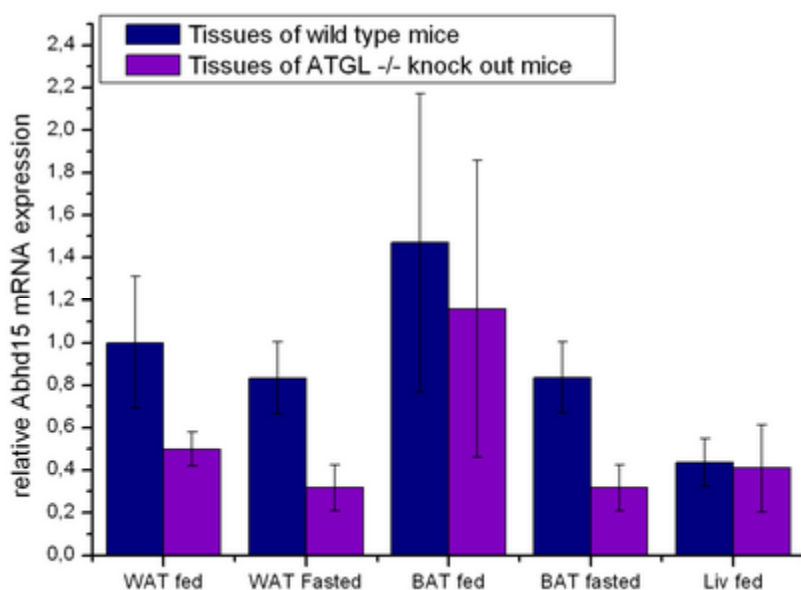


Figure 24: Comparison of *Abhd15* expressions in *Atgl* knockout and wild type murine tissues

Because of these results it can be assumed that *Atgl* somehow has influence on the regulation of *Abhd15* expression but not required. Furthermore it is unlikely that ABHD15 takes over the TG degradation implemented by ATGL.

To investigate whether ABHD15 shows phospholipase activity, cos7 cells overexpressing histidin-tagged *Abhd15* were used. For this purpose the pHisMaxC-*Abhd15* construct was prepared as mentioned before. After ligation of the *Abhd15* gene, equipped with a forward *Bam*HI and a reverse *Xho*I restriction site by PCR (electrophoresis gel of double digested vector and insert see figure 25a) into the pHisMaxC vector, a transformation into *E. coli* Top10 cells was done, providing nine ampicillin resistant colonies. The following control restrictions identified all nine colonies as positive pHisMaxC-*Abhd15* constructs. Control digestion of the miniprep DNAs with *Bam*HI and *Xho*I showed that the *Abhd15* gene (1.4 kbp) was inserted into all HisMaxC plasmids (5.3 kbp). A further control digestion was done with *Bgl*II and *Xho*I resulting in one fragment of 4.0 kbp and one fragment of 2.6 kbp, which

4 Results

proved the results of the first restriction digest (figure 25b). For better understanding of the exonuclease digests the vector map of the plasmid including the *Abhd15* insert is shown in figure 25c.

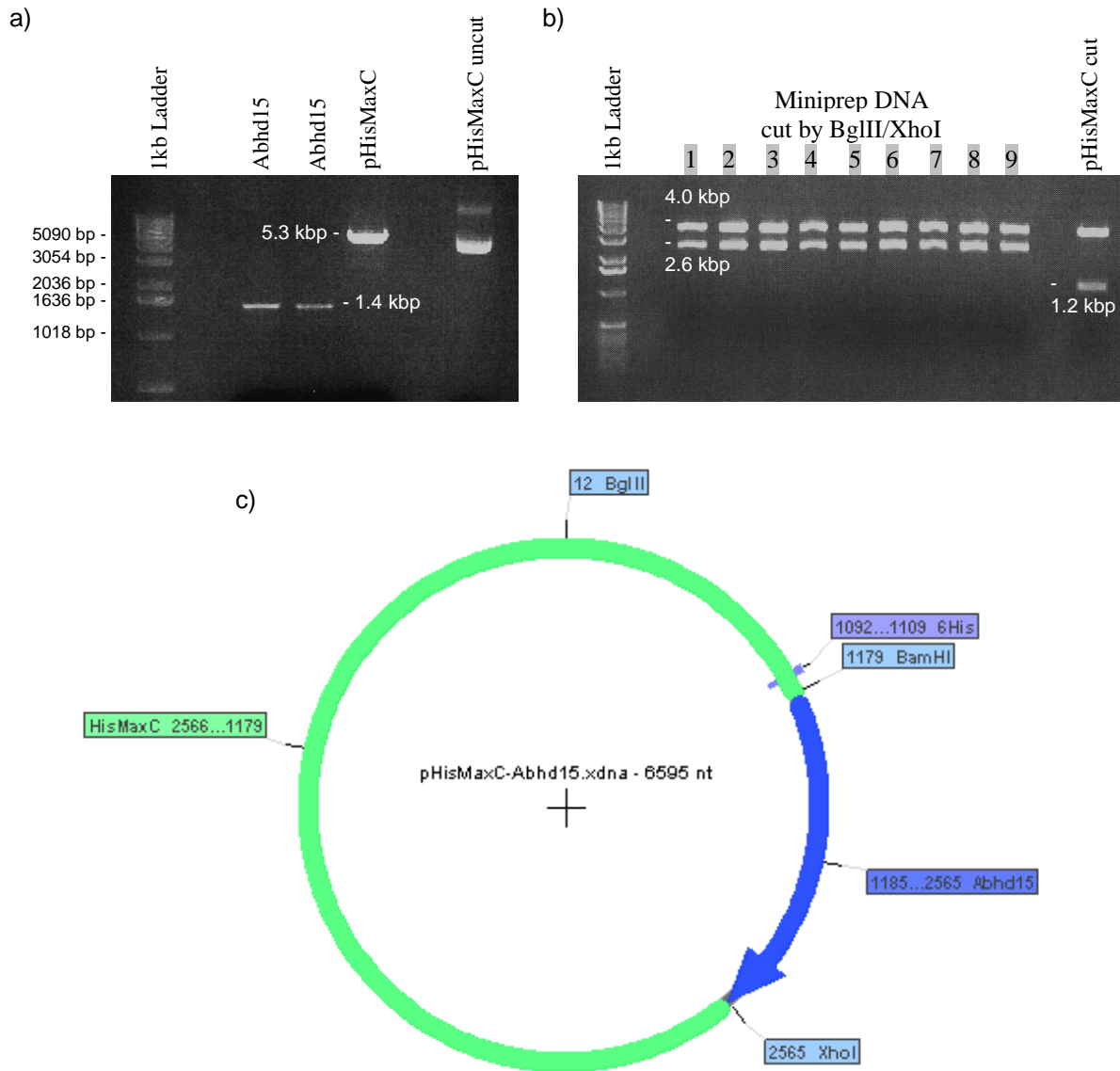


Figure 25: Electrophoresis gels of *pHisMaxC-Abhd15* preparation and vector map of *pHisMaxC-Abhd15*, including restriction sites for control cuts

After transfection of *cos7* cells with a *pHisMaxC-Abhd15* construct and *pHisMaxC* as a control, the cells were reaped 72 hours later and proteins isolated and measured as described before. Expression of the ABHD15 protein in the cells was confirmed by western blot analysis using an anti-His antibody.

To measure the hydrolase activity of ABHD15, cell lysates from control and *Abhd15*-overexpressing cells were incubated with two different phosphatidylcholins (PC) and the release of free fatty acids (FFA) was determined (figure 26).

4 Results

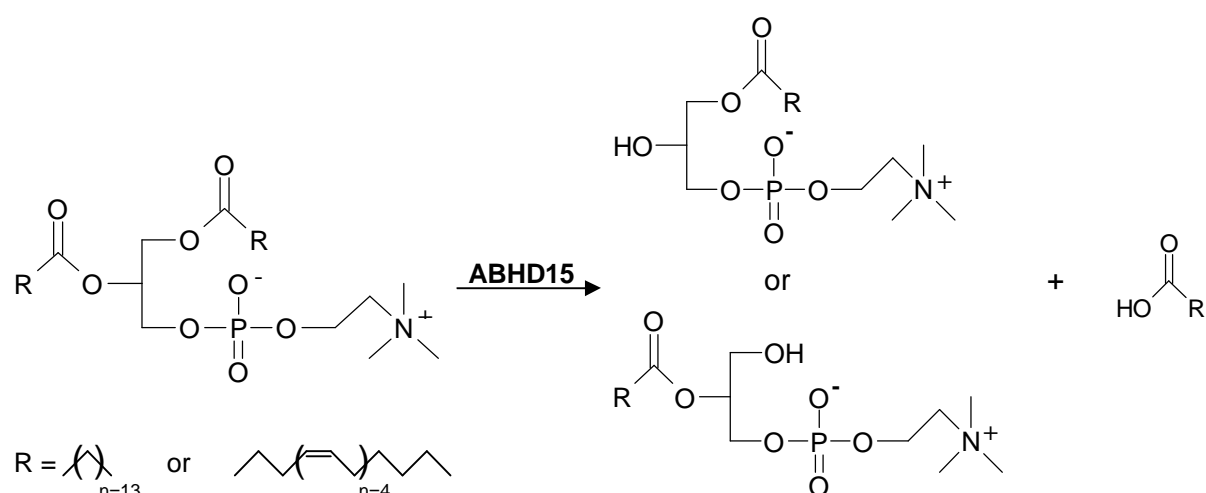


Figure 26: Equation of possible activities of ABHD15

Incubation of dipalmitic- or diarachidonic-phosphatidylcholine with *Abhd15*-overexpressing *cos7* cell lysates doubled the release of FFA from the according PC in comparison to control cell lysates. The release of FFA was detected by the NEFA-HR (2) test (data not shown). These results show that ABHD15 acts as a phospholipase.

4.8 ABHD15 locates to the endoplasmic reticulum and is secreted

To evaluate the subcellular localization of ABHD15, *pHisMaxC-Abhd15* overexpressing *cos7* cells and control cells were fractionated by centrifugation and ABHD15-protein expression in the various fractions was examined by western blotting. Western blot analysis showed that there is no ABHD15 (51.2 kDa) in the cytoplasm (figure 27), whereas it could be found in the membrane containing fraction. The ABHD15 band, which is visible in the nuclei fraction, probably can be ascribed to impurity (shown below).

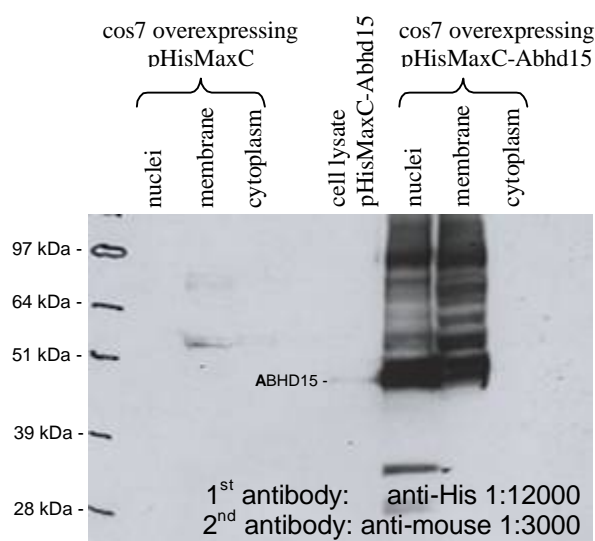


Figure 27: Subcellular localization of ABHD15 in *pHisMaxC-Abhd15* overexpressing *cos7* cells

4 Results

To receive the location of ABHD15 in pHisMaxC-*Abhd15* overexpressing cos7 cells in more detail, immunofluorescence experiments using an antibody against N-terminal His-Tag were carried out. It could be shown that ABHD15 was mainly located to the endoplasmatic reticulum (ER) as demonstrated by double immunostaining of ABHD15 (figure 28a) and the ER marker D1er (figure 28b). The merged images show a significant overlap of the red and green (because of the YFP of D1er) signal (figure 28d). Compared with the DAPI blue coloured nucleus it can be said that there is no ABHD15 inside the cell nucleus (figure 28c).

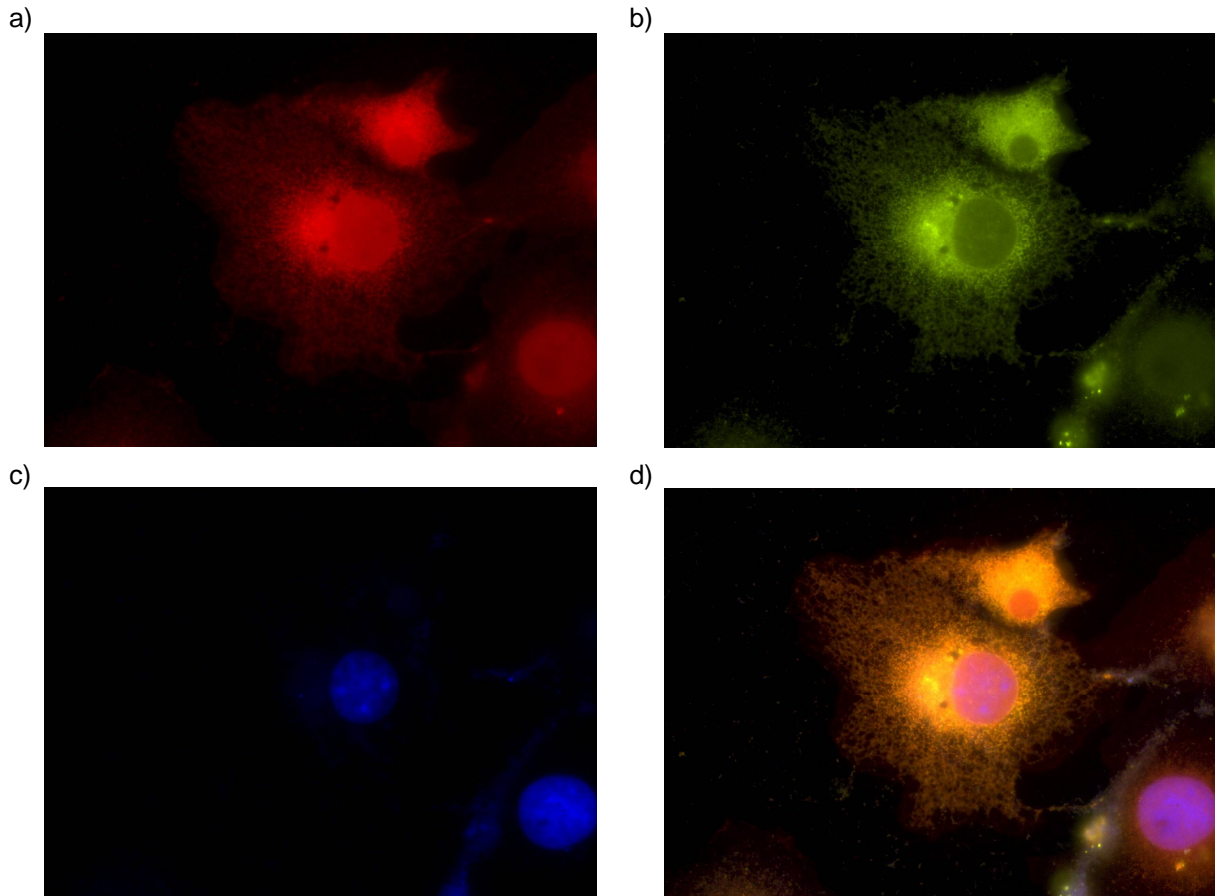


Figure 28: Immuno labelling of ABHD15 (red), D1er (green), and the nucleus (blue), reveals that ABHD15 locates to the ER

Furthermore, it was investigated whether ABHD15 is secreted and can be detected in the media of *Abhd15*-overexpressing cos7 cells. However, as mentioned before, an N-terminal signal peptide region is predicted from amino acid 1-28. Taking into account that signal sequences are split off very often, a new construct was designed, equipped with a C-terminal His-Tag for western blotting. The His-Tag was added C-terminally by PCR, altogether with a forward *Bgl*II and a reverse *Xho*I restriction site. After ligation of the PCR product into the MSCVpuro plasmid a transformation into Top10 cells was done, providing 15 ampicillin resistant colonies. The following control restriction with *Bgl*II and *Hind*III identified five colonies as pMSCVpuro-*Abhd15*-His-Tag constructs containing, as they showed one

4 Results

fragment of 5.8 kbp and a second fragment with 1.9 kbp instead of 0.5 kbp that would be cut out of the empty vector (figure 29).

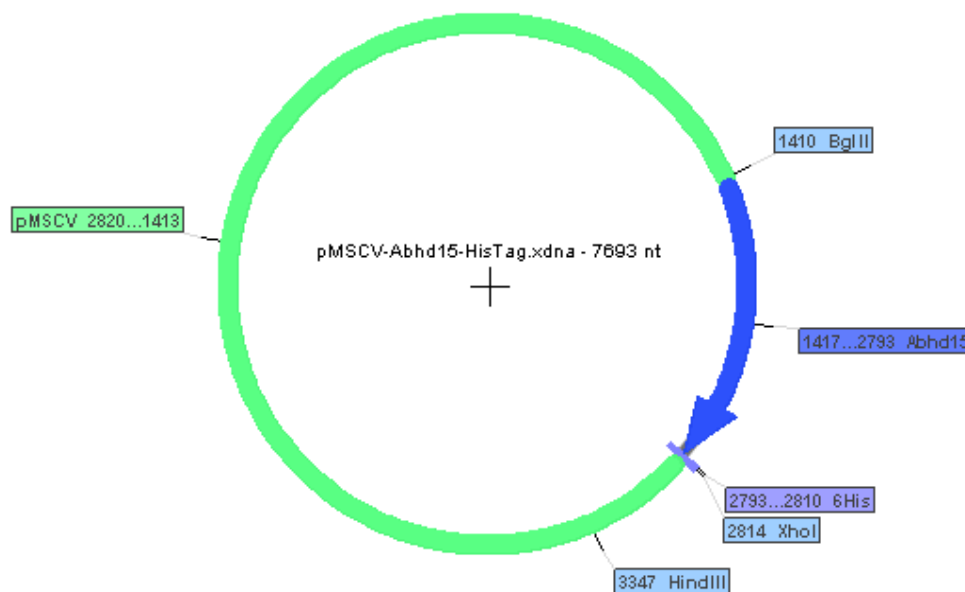
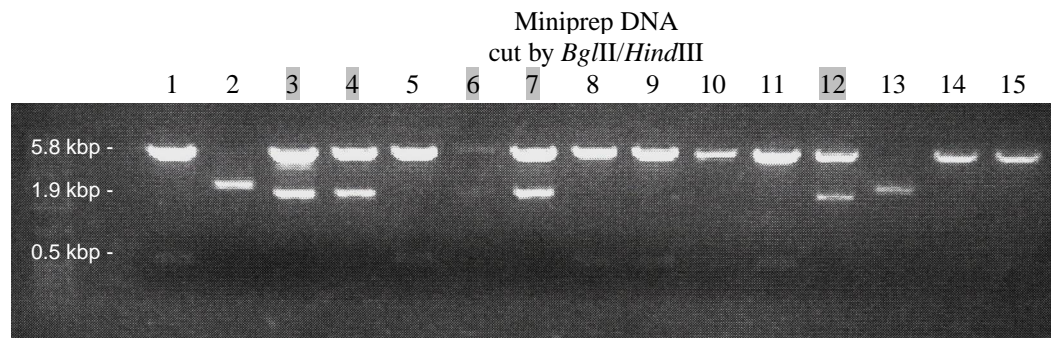


Figure 29: Control restriction enzyme double digest of pMSCVpuro-*Abhd15*-His-Tag Miniprep DNA by *Bgl*III/*Xho*I and pMSCVpuro-*Abhd15*-His-Tag vector map, including the restriction sites for control cuts

The gathered cell lysate and the supernatant of pMSCVpuro-*Abhd15*-His-Tag overexpressing cos7 cells were evaluated by western blotting using a His-Tag antibody as described before. Unfortunately, no ABHD15 bands became visible, although the mRNA expression of *Abhd15* was increased, which was controlled by qPCR.

Notwithstanding the negative predictions about the probably cleaved N-terminal His-Tag of the pHisMaxC-*Abhd15* construct, the cell lysate as a positive control, and the supernatant of pHisMaxC-*Abhd15*-overexpressing cos7 cells were used for western blotting as described before. Interestingly, there was definitely ABHD15 protein expression in the cell supernatant of *Abhd15*-overexpressing cos7 cells, which proves that ABHD15 is secreted with the signal peptide (figure 30).

4 Results

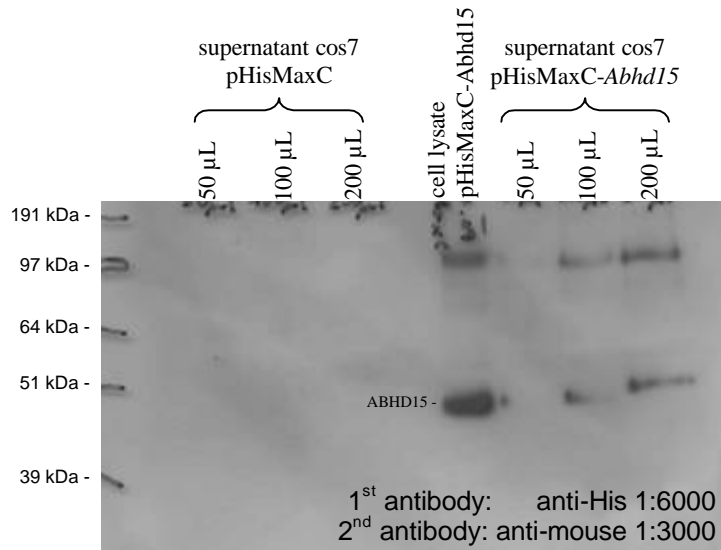


Figure 30: Western blot of secreted ABHD15 of pHisMaxC-*Abhd15* overexpressing cos7 cells

If not otherwise stated results are mean values (\pm standard deviation) of at least two independent experiments or results show one representative experiment.

* $p = 0.05$, ** $p = 0.001$

5 Discussion

To start with, possible functions of ABHD15 were perceived by comparing the predicted protein domains of ABHD15 sequence with other, better understood and functionally described genes. This database search reduced the wide spread possible applications of a hydrolase, which ranges from dehydrogenases, to dehalogenases, to peroxidases and so on, to a lipase or esterase activity. The prediction of this activity gave the hint to an important involvement in lipolysis and thus to a probable involvement in adipogenesis, which had to be proved.

The examined regulation of the mRNA expression during adipocyte differentiation in various murine cell lines, which turned out to be the most suitable experimental model (figure 9), showed the connection of *Abhd15* to adipogenesis. It could be shown that the gene is highly expressed during the late phase of the terminal adipogenic differentiation and slightly downregulated afterwards (figures 11 and 12), which means similar expression behaviour as for *Ppar γ* and *C/ebp α* . Hence to the roles of PPAR γ and C/EBP α , it can be assumed that likely ABHD15 plays a role in the late differentiation as well as in the maintenance of the differentiated status of adipocytes. ABHD15 was not only strongly upregulated in murine cells that undergo adipogenesis, but also in human SGBS cells. Thus ABHD15 also might play an important role in human adipocyte differentiation and therefore could be a target gene in the process of fat cell development and further for the treatment of obesity.

A further hint for an important role in adipogenesis is the expression profile of *Abhd15* mRNA in murine tissues. The gene is highly expressed in the brown (BAT) and the white adipose tissue (WAT), whereas it is expressed to a lower extent in the liver and hardly found in skeletal (SM) and cardiac muscle (CM), where only small amounts of lipid droplets are found under normal, healthy conditions. This allocation is suitable for the assumption that ABHD15 plays a role in adipogenesis, as *Abhd15* mRNA expression is high in WAT and BAT in comparison to SM and CM in accordance with the amounts of fat. However, the investigation of genetically obese mice (*ob/ob*), which do not produce leptin and therefore never feel satiety, showed a doubling of the *Abhd15* mRNA expression only in liver, but not in WAT (figure 14). This result does not fit well to the expectation of an increase of ABHD15 expression upon accumulation of fat. Thus it remains questionable whether ABHD15 does play a direct role in the formation of lipid droplets.

Furthermore it was investigated if food accessibility or different diets influence *Abhd15* mRNA expression (figure 15). The fact that fasted mice show a slight decrease of *Abhd15* expression makes a propellent role of *Abhd15* in lipogenesis more likely than in lipolysis, as a degrading role, to make energy available in times of energy demand, would be enlightened by an increase of *Abhd15* mRNA in fasted mice. Further the expression of *Abhd15* in mice either genetically obese or challenged with a high fat diet (HFD) was investigated. Usually particularly lipases and enzymes, which convert fat nourishment into utilizable metabolites,

5 Discussion

are upregulated in obese mice or mice on a HFD. However, neither the expression of *Abhd15* mRNA of genetically obese mice nor that of mice on a HFD showed any increase in WAT, which concludes no influence on free fatty acid (FFA) release from triglycerides (TG). Furthermore, the expression of *Abhd15* under various conditions *in vitro* was controlled. As there was shown that *Abhd15* is upregulated during adipogenic differentiation in 3T3-L1 cells, the influences of the components of the induction cocktail on their own were tested. The addition of IBMX, which acts as a cAMP inhibitor, did not change the *Abhd15* mRNA expression, whereas the addition of insulin (Ins) or dexamethasone (Dex) resulted in a small increase (figure 16). Ins has a wide field of application, as it promotes lipogenesis and inhibits lipolysis^{8,11}. Dex, which is a glucocorticoid, also shows a wide spread application area, which includes activation of C/EBP δ expression, for example. In general glucocorticoids are known for their interventions on carbohydrate, protein and lipid metabolism as well⁷. All together it is very unlikely that Ins or Dex have direct effects onto *Abhd15* expression, as the increases of expression are very small.

As far as the expression pattern of *Abhd15* is similar to the one of *Ppar γ* during 3T3-L1 adipogenic differentiation, direct targeting of *Abhd15* by PPAR γ or the other way around was evaluated. To investigate if there are any influences of PPAR γ on *Abhd15* mRNA expression, the PPAR γ agonist Rosi was added for different times and in different doses to fully differentiated cells. As a result, a time but not dose dependent increase of *Abhd15* expression, induced by PPAR γ activation could be observed (figure 18). There may be various reasons for the time, but not dose dependence of the increased *Abhd15* expression. One explanation for the time dependence is that PPAR γ needs time to reach the point of activation of *Abhd15*, another could be that Rosi needs time to reach the PPAR γ binding sites. As the increased expression of the *Abhd15* mRNA is not further increased from 1 μ M to 5 μ M Rosi, it might be that the 1 μ M concentration is already sufficient to cover either all PPAR γ binding sites or to cover all ABHD15 binding sites for PPAR γ . For this reason more dose dependency studies with lower Rosi concentrations should be done down the road. Moreover, studies of *Ppar γ* knockout (ko) MEFs showed that *Abhd15* is expressed only in the presence of *Ppar γ* . Additionally Rosi can increase *Abhd15* expression only if *Ppar γ* expression is possible, as far as the addition of Rosi could not overcome the missing *Abhd15* expression in *Ppar γ* double ko MEFs (figure 19). Summarizing it can be said that *Abhd15* is definitely a PPAR γ target, but the point of action has to be studied in more detail by the use of ChIP-qPCR and luciferase reporter assays.

To show the importance of ABHD15 in *in vitro* models, the gene was silenced by the use of shRNA. As this application did not work properly, more focus was laid onto the stable overexpression of *Abhd15*. The 200-fold increased *Abhd15* mRNA expression of *Abhd15*-overexpressing 3T3-L1 cells further increases after addition of the standard induction cocktail

5 Discussion

compared to control cells. But this increased *Abhd15* expression does not lead to any obvious morphological changes in neither condition (figure 23). Thus, the increased expression of *Abhd15* mRNA does not evoke an increased lipid droplet formation neither before nor upon induction with the standard induction cocktail. On one hand this could be a hint that ABHD15 is not involved in lipid droplet formation, on the other hand an increased *Abhd15* mRNA expression does not mean automatically an increased amount of translated proteins. The examination of the induction cocktail ingredients in particular brought up an unexpected result. In contrast to IBMX and Ins, which do not influence *Abhd15* expression, the addition of Dex alone leads to a nearly 600-fold increased expression of *Abhd15* in 3T3-L1 cells already overexpressing *Abhd15* stably. This increase was even higher than the one reached upon addition of Rosi to the standard induction cocktail. Thus, in 3T3-L1 cells overexpressing *Abhd15* stably, Rosi does not lead to a further increase of *Abhd15* expression in comparison to control 3T3-L1 cells that were induced with the standard hormonal cocktail and Rosi. A reason for this could be that further increased expression would not be bearable for the cells, so that even additional PPAR γ activation does not lead to a further increase of *Abhd15* expression. Anyhow, the treatment with Dex led to *Abhd15* mRNA expression levels which forced the cells to differentiate very fast, but die immediately afterwards. It is difficult to name the reason for this different reaction of the *Abhd15* overexpressing cells compared to control cells. As there is only a small effect upon addition of Dex onto the *Abhd15* mRNA expression in normal expressing cells, *Abhd15* is unlikely a direct target of Dex. It is only known that Dex activates the early transcription factor C/EBP δ , which subsequently induces *Ppar γ* expression. It may be that *C/ebp δ* is expressed long before *Abhd15* in 3T3-L1 cells not overexpressing *Abhd15*. Hence, Dex activates C/EBP δ , but there is hardly any *Abhd15* mRNA expression that could be transactivated further by C/EBP δ . Thus, upon overexpression of *Abhd15*, Dex-activated C/EBP δ finds enough *Abhd15* target for transactivation. Another explanation could be sterical reasons, which prevent C/EBP δ and/or PPAR γ to activate or increase *Abhd15* expression directly. In this case a higher gene number of *Abhd15* would rise the probability of liaison. This would bring up a “back coupling”. However, this huge effect of Dex does not appear when Dex is added in combination with IBMX and Ins in the standard induction cocktail. A reason therefore could be that Ins influences the carbohydrate, protein and lipid metabolism vice versa glucocorticoids do⁷ and therefore neutralize the effect of Dex. Anyway, the detailed mode of operation of Dex is not known by now.

However, *Abhd15* seems to be involved in adipogenesis as a PPAR γ target, but how ABHD15 effects adipogenesis stays in shadow until now. To start with this quest it was necessary to examine the function of the protein. As there was predicted an esterase or lipase function, and lipases are well known to be involved in adipogenesis, ABHD15 was

5 Discussion

tested for lipase activities. First a TG lipase activity was assumed, because lipid droplets consist of TGs. Anyhow, one might hypothesize that ABHD15 has no TG lipase function, as it is not upregulated in ATGL-ko mice to take over the TG lipase activity (figure 24). However, it turned out that ABHD15 shows phospholipase activity, which opens a wide field of application and brings up the question whether the degradation of a substrate or the production of special metabolites is the important event in adipogenesis. Phospholipids are commonly known for their membrane function, which could give ABHD15 the possibility to interfere in membranes. On the other hand it turned out that ABHD15 is localized at the ER and secreted afterwards. This fact makes the possibility of an interaction with lipoproteins more likely.

A famous group of phospholipase, in which ABHD15 fits in very well, is the group of the phospholipases A₂ (PLA₂), which also includes some secreted ones (sPLA₂). Members of this group hydrolyse phospholipids on the *sn*-2 position of membrane glycerophospholipids and hence produce lysophospholipids and FFAs. Some of these metabolites are very important for adipogenesis. Lysophospholipides, for example, sometimes are biologically active by themselves, or are precursors for bioactive mediators. A very important FFA is arachidonic acid, which is the source for all natural PPAR_γ ligands, like eicosanoids. Hence to these important products, PLA₂ are very important for signalling and membrane remodelling³⁴ and moreover influence PPAR_γ, C/EBP_α, C/EBP_β and C/EBP_δ³⁵.

This thesis brought up very interesting facts about *Abhd15*, but there are still many steps to be done to elucidate all properties of this gene and its protein function. Anyhow it can be said that ABHD15 plays an important role in adipogenesis and due to the fact that it is secreted ABHD15 gives a great point of interest for potential medication against the global problem of obesity.

6 Figure Legends

Figure 1: Adapted scheme of whole process of adipogenesis ⁸	9
Figure 2: Draft of the transcriptional cascade in the terminal adipocyte differentiation ⁶	10
Figure 3: Diagram of the secondary structure of the "canonical α/β hydrolase" fold ²⁷	12
Figure 4: Vector maps of cloning plasmids pMSCVpuro and pHisMaxA,B,C	20
Figure 5: Temperature program for PCR	21
Figure 6: Temperature program for qPCR	25
Figure 7: Construction for wet western blot transfer	27
Figure 8: Phylogenetic tree of <i>Abhd15</i> cDNA of different mammals	30
Figure 9: Phylogenetic tree of <i>Abhd15</i> cDNA of humans, mice, and rats	30
Figure 10: Predicted superfamily and signal peptide (Sig) domains of ABHD15	30
Figure 11: <i>Abhd15</i> expression during differentiation of (a) 3T3-L1 fibroblasts, (b) OP9 cells and (c) MEFs	31
Figure 12: <i>Abhd15</i> expression during differentiation of SGBS cells	32
Figure 13: Expression of <i>Abhd15</i> in murine tissues	32
Figure 14: Expression of <i>Abhd15</i> in WAT and Liv of wild type and genetically obese (ob/ob) mice	33
Figure 15: Comparison of <i>Abhd15</i> expression in mice on various diets	33
Figure 16: <i>Abhd15</i> expression after 7 days of treatment of 3T3-L1 cells with various additives	34
Figure 17: <i>Abhd15</i> expression during differentiation with and without addition of Rosi (1 μ M)	35
Figure 18: <i>Abhd15</i> expression during short term treatment of fully differentiated 3T3-L1 cells with Rosi	35
Figure 19: <i>Abhd15</i> expression in <i>Pparγ</i> ^{-/-} and +/- MEFs	36
Figure 20: <i>Abhd15</i> expression of <i>Abhd15</i> silenced cells during differentiation	37
Figure 21: Electrophoresis gels of pMSCVpuro- <i>Abhd15</i> preparation	38
Figure 22: Vector map of the pMSCVpuro- <i>Abhd15</i> construct, including the restriction sites for control cuts	38
Figure 23: Stable overexpression of (a) pMSCVpuro and (b) pMSCVpuro- <i>Abhd15</i> in 3T3-L1 cells treated with different media for 8 days	39

6 Figure Legends

Figure 24: Comparison of <i>Abhd15</i> expressions in <i>Atgl</i> knockout and wild type murine tissues	40
Figure 25: Electrophoresis gels of pHisMaxC- <i>Abhd15</i> preparation and vector map of pHisMaxC- <i>Abhd15</i> , including restriction sites for control cuts	41
Figure 26: Equation of possible activities of ABHD15	42
Figure 27: Subcellular localization of ABHD15 in pHisMaxC- <i>Abhd15</i> overexpressing cos7 cells	42
Figure 28: Immuno labelling of ABHD15 (red), D1er (green) and the nucleus (blue) reveals that ABHD15 locates to the ER	43
Figure 29: Control restriction enzyme doubledigest of pMSCVpuro- <i>Abhd15</i> -His-Tag Miniprep DNA by <i>BglII/XhoI</i> and pMSCVpuro- <i>Abhd15</i> -His-Tag vector map, including the restriction sites for control cuts	44
Figure 30: Western blot of secreted ABHD15 of pHisMaxC- <i>Abhd15</i> overexpressing cos7 cells	45

7 References

1. K. M. FLEGAL, M. D. CARROL, C. L. OGDEN, and C. L. JOHNSON. Prevalence and trends in obesity among US adults, 1999-2000. *JAMA* 288: 1723-1727, 2000
2. P. G. KOPELMAN. Obesity as a medical problem. *Nature* 404: 635-643, 2000
3. B. M. SPIEGELMANN, and J. S. FLIER. Obesity and the regulation of energy balance. *Cell* 104: 531-543, 2001
4. J. M. FRIEDMAN. Obesity in the new millenium. *Nature* 404: 632-634, 2000
5. S. MANDRUP, and M. D. LANE. Regulating adipogenesis. *J. Biol. Chem.* 272: 5367-5370, 1997
6. E. D. ROSEN, and O. A. MACDOUGALD. Adipocyte differentiation from the inside out. *Nat. Rev. Mol. Cell Biol.* 12: 885-96, 2006
7. D. VOET, and J. G. VOET. Biochemie. VCH
8. F. M. GREGOIRE, C. M. SMAS, and H. S. SUL. Understanding adipocyte differentiation. *Phys. Rev.* 78: 783-809, 1998
9. L. A. CAMPFIELD, F. J. SMITH, and P. BURN. The OB protein (leptin) pathway – a link between adipose tissue mass and central neural networks. *Horm. Metab. Res.* 28: 619-632, 1996
10. E. D. ROSEN, C. J. WALKEY, P. PUIGSERVER, and B. M. SPIEGELMAN. Transcriptional regulation of adipogenesis. *Genes Dev.* 14: 1293-1307, 2000
11. P. CORNELIUS, O. A. MACDOUGALD, and D. LANE. Regulation of adipocyte development. *Annu. Rev. Nutr.* 14: 99-129, 1994
12. Z. WU, N- L. BUCHER, and S. R. FARMER. Induction of peroxisome proliferator-activated receptor gamma during conversion of 3T3-L1 fibroblasts into adipocytes is mediated by C/EBPdelta, and glucocorticoids. *Mol. Cell Biol.* 16: 4128-4136, 1996
13. C. M. CONSTANCE, J. I. IV MORGAN, and R. M. UMEK. C/EBPalpha regulation of the growth-arrest-associated gene gadd45. *Mol. Cell. Biol.* 16: 3878-3883, 1996
14. N. A. TIMCHENKO, M. WILDE, M. NAKANISHI, J. R. SMITH, and G. J. DARLINGTON. CCAAT/enhancer binding protein α (C/EBP α) inhibits cell proliferation through the p21 (WAF-1/CIP-1/SDI-1) protein. *Genes Dev.* 10: 804-815, 1996
15. J. AUVERX. PPARgamma, the ultimate thrifty gene. *Diabetologia* 42: 1033-1049, 1999
16. R. J. PERERA, E. G. MARCUSSON, S. KOO, X. KANG, Y. KIM, N. WHITE, and N. M. DEAN. Identification of novel PPAR γ target genes in primary human adipocytes. *Gene* 15: 90-99, 2006
17. E. D. ROSEN, and B. M. SPIEGELMAN. PPAR γ : a nuclear regulator of metabolism, differentiation, and cell growth. *J. Biol. Chem.* 41: 37731-37734, 2001
18. T. M. MCINTYRE, A. V. PONTSLER, A. R. SILVA, A. ST. HILAIRE, Y. XU, J. C. HINSHAW, G. A. ZIMMERMAN, K. HAMA, J. AOKI; H. ARAI, and G. D.

7 References

- PRESTWICH. Identification of an intracellular receptor for lysophosphatidic acid (LPA): LPA is a transcellular PPAR γ agonist. *Proc. Natl. Acad. Sci. USA* 100: 131-136, 2003
19. P. TONTONOZ, R. A. GRAVES, A. I. BUDAVARI, H. ERDJUMENT-BROMAGE, M. LUI, E. HU, P. TEMPST, and B. M. SPIEGELMAN. Adipocyte-specific transcription factor ARF6 is a heterodimeric complex of two nuclear hormone receptors, PPAR γ and RXR α . *Nucl. Acids Res.* 22: 5628-5634, 1994
20. M. LEHRKE and M. A. LAZAR. The many faces of PPAR γ . *Cell* 123: 993-999, 2005
21. E. J. GOETZL, H. LEE, H. DOLEZALOVA, K. R. KALLI, C. A. CONOVER, Y. L. HU, T. AZUMA, T. P. STOSSEL, J. S. KARLINER, and R. B. JAFFE. Mechanisms of lysolipid phosphate effects on cellular survival and proliferation. *Ann. N.Y. Acad. Sci.* 905: 177-187, 2000
22. R. P. BRUN, J. B. KIM, E. HU, S. ALTIOK, and B. M. SPIEGELMAN. Adipocyte differentiation: a transcriptional regulatory cascade. *Curr. Opin. Cell Biol.* 8:826-832, 1996
23. A. PROKESCH, H. HACKL, R. HAKIM-WEBER, S. R. BORNSTEIN and Z. TRAJANOSKI. Novel insight into adipogenesis from omics data. *Curr. Med. Chem.* 16: 2952-2964, 2009
24. H. HACKL, T. R. BURKARD, A. STURN, R. RUBIO, A. SCHLEIFFER, S. TIAN, J. QUACKENBUSH, F. EISENHABER, and Z. TRAJANOSKYI. Molecular processes during fat cell development revealed by gene expression profiling and functional annotation. *Genome Biol.* 6: R108, 2005
25. P. CARNICI and Y. HAYASHIZAKI. High-efficiency full-length cDNA cloning. *Methods Enzymol.* 303: 19-44, 1999
26. P. CARNICI et al., FANTOM Consortium; RIKEN Genome Exploration Research Group and Genome Science Group (Genome Network Project Core Group). The transcriptional landscape of the mammalian genome. *Science* 309: 1559-1563, 2005
27. D. L. OLLIS, E. CHEAH, M. CYGLER, B. DIJKSTRA, F. FROLOW, S. M. FRANKEN, M. HAREL, S. J. REMINGTON, I. SILMAN, J. SCHRAG, et al. The α/β hydrolase fold. *Protein Eng.* 5: 197-211, 1992
28. M. NARDINI and B. W. DIJKSTRA. α/β Hydrolase fold enzymes: the family keeps growing. *Curr. Opin. Struct. Biol.* 9: 732-737, 1999
29. E. SMIRNOVA, E. B. GOLDBERG, K. S. MAKAROVA, L. LIN, W. J. BROWN, and C. L. JACKSON. ATGL has a key role in lipid droplet/adiposome degradation in mammalian cells. *EMBO Rep.* 7: 106-113, 2006

7 References

30. R. ZIMMERMANN, J. G. STRAUSS, G. HAEMMERLE, et al. Fat mobilization in adipose tissue is promoted by adipose triglyceride lipase. *Science* 306: 1383-1386, 2004
31. G. HAEMMERLE, R. ZIMMERMANN, and R. ZECHNER. Letting lipids go: hormone-sensitive lipase. *Curr. Opin. Lipidol.* 14: 289-297, 2003
32. P. FISCHER-POSOVSKY, F. S. NEWELL, M. WABITSCH, and H. E. TORNQUIST. Human SGBS cells – a unique tool for studies of human fat cell biology. *Obes. Facts* 1: 184-189, 2008
33. M. I. LEFTEROVA, Y. ZHANG, D. J. STEGER, M. SCHUPP, J. SCHUG, A. CRISTANCHO, D. FENG, D. ZHUO, C. J. Jr. STOECKERT, X. S. LIU, and M. A. LAZAR. PPAR γ and C/EBP factors orchestrate adipocyte biology via adjacent binding on a genome-wide scale. *Genes Dev.* 22: 2941-2952, 2008
34. I. KUDO, and M. MURAKAMI. Phospholipase A₂ enzymes. *Prostaglandins Other Lipid Mediat.* 68-69: 3-58, 2002
35. X. SU, S. J. MANCUSO, P. E. BICKEL, C. M. JENKINS, and R. W. GROSS. Small interfering RNA knockdown of Calcium-independent Phospholipases A₂ β or γ inhibits the hormone-induced differentiation of 3T3-L1 preadipocytes. *J. Biol. Chem.* 279: 21740-21748, 2004
36. J.M. FRIEDMAN and J. L. HALAAS. Leptin and the regulation of body weight in mammals. *Nature* 395: 763-770, 1998
37. W. H. MOOLENAAR. Lysophosphatidic acid, a multifunctional phospholipid messenger. *J. Biol. Chem.* 270: 12949-12952, 1995
38. G. PAGES, A. GIRARD, O. JEANNETON, P. BARBE, C. WOLF, M. LAFONTAN, P. VALET, and J. S. SAULNIER-BLANCHE. LPA as a paracrine mediator of adipocyte growth and function. *Ann. N.Y. Acad. Sci.* 905: 159-164, 2000